

LOW TEMPERATURE BATTERY MONITORING AND CONTROL SYSTEM – LITHIUM-ION LOW TEMPERATURE CASE STUDY

by

Aaron Lee, Richard Tham, Ken Huynh

Senior Project

ELECTRICAL ENGINEERING DEPARTMENT

California Polytechnic State University

San Luis Obispo

2014

Table of Contents

	Page
List of Figures and Tables.....	i
Abstract.....	iii
I. Introduction.....	1
II. Initial Requirements and Specifications.....	2
III. Initial Functional Decomposition (Level 0 and Level 1)	4
IV. Final Requirements and Specifications.....	6
V. Final Functional Decomposition (Level 0 and Level 1).....	7
VI. Internal Impedance Monitor Design	9
A. Excitation Circuit.....	9
i. Design.....	9
ii. Test	12
B. Amplifier Circuit	12
i. Design.....	12
ii. Test	14
C. Completed Design	15
i. Design.....	15
ii. Test	17
VII. Internal Impedance Monitor PCB	20
A. Design.....	20
B. Test	21
C. PCB Freeze Test.....	21
VIII. Lithium-Ion Battery Tests	23
A. Room Temperature Impedance Characterization Tests.....	23
B. Temperature Sweep Impedance Sweep Tests.....	24
C. Discharge Tests.....	27
D. Knee Tests	29
IX. Conclusion	32

X. References	33
---------------------	----

Appendices

A. Senior Project Analysis	34
----------------------------------	----

List of Figures and Tables

Table

1. Initial System Requirements and Specifications	2
2. Initial Level 0 System Functional Requirements	4
3. Level 1 Subsystem - Impedance Monitor Functional Requirements.....	5
4. Level 1 Subsystem - Control Block Functional Requirements	5
5. Final System Requirements and Specifications.....	6
6. Final Level 0 System Functional Requirements.....	7
7. Level 1 Subsystem – Excitation Circuit Functional Requirements	8
8. Level 1 Subsystem – Amplifier Circuit Functional Requirements.....	8
9. Average Output Voltages of Lock-In Amplifier at Varying Chopping Mixer Frequencies.....	24
10. Knee Test Results.....	31
11. Labor Cost Estimates.....	35
12. Parts Cost Estimates Breakdown (Estimate)	35
13. Parts Cost Estimates	36
14. Actual Parts Costs	36
15. Project Timeline (Gantt Chart).....	39

Figures

1. Initial Level 0 Block Diagram.....	4
2. Initial Level 1 Block Diagram.....	5
3. Final Level 0 Block Diagram	7
4. Final Level 1 Block Diagram	7
5. Battery Internal Impedance Model.....	8
6. Generic Lock-In Amplifier Schematic	9
7. Initial Excitation Circuit - LC Circuit	10
8. Final Excitation Circuit - 555 Timer Circuit	10
9. 555 Timer Circuit Transient Simulation.....	11
10. 555 Timer Circuit Experimental DIS Waveform	12
11. Discrete Amplifier Schematic	12

12. Frequency Response of Discrete Amplifier.....	13
13. Chopping Mixer Schematic.....	13
14. Buffered Low-Pass Filter Schematic.....	14
15. Discrete Amplifier Gain @ 1 kHz; green = output, yellow = input	14
16. Complete Lock-In Amplifier Design for Battery Internal Impedance Measurements	15
17. Lock-In Amplifier Transient Simulation - Key Waveforms	15
18. Lock-In Amplifier Steady-State DC Output Simulation	16
19. $r_{in} = 28.8 \Omega$ – Ch.1 = Output of Discrete Amplifier; Ch.2 = 555 Timer DIS Pin.....	17
20. $r_{in} = 28.8 \Omega$ – Ch.1 = Drain of MOSFET for Chopping Mixer; Ch.2 = Output of Chopping Mixer....	17
21. $r_{in} = 28.8 \Omega$ – Output DC Voltage of Lock-In Amplifier	18
22. $r_{in} = 103 \Omega$ – Ch.1 = Output of Discrete Amplifier; Ch.2 = 555 Timer DIS Pin.....	18
23. $r_{in} = 103 \Omega$ – Ch.1 = Drain of MOSFET for Chopping Mixer; Ch.2 = Output of Chopping Mixer....	19
24. $r_{in} = 103 \Omega$ – Output DC Voltage of Lock-In Amplifier	19
25. Impedance Monitor PCB Artist Schematic	20
26. Impedance Monitor PCB Layout.....	20
27. PCB Temperature Sweep Test Results.....	22
28. Lock-in Output vs. Frequency of Batteries at Room Temperature	23
29. A5 Impedance vs. Temperature Test Results	25
30. A7 Impedance vs. Temperature Test Results	26
31. B5 Impedance vs. Temperature Test Results	26
32. B9 Impedance vs. Temperature Test Results	27
33. $T = -28.8^\circ\text{C}$ - Ch.1 - Output of Discrete Amplifier; Ch. 2 - DC Output Voltage (Battery A7).....	27
34. $T = -52^\circ\text{C}$ - Ch. 1 - Output of Discrete Amplifier; Ch. 2 - DC Output Voltage (Battery A7)	28
35. A-Type (3400 mAh rated) Discharge Test Results	29
36. B-Type (3100 mAh rated) Discharge Test Results	30
37. Example of "Knee" Area for Knee Test Results	31

Abstract

This open-ended research project, co-advised by Dr. Prodanov and Dr. Dolan, studies electronic and battery failures at low temperatures (between -70 °C to 0 °C). The main battery technology used for this project is Lithium-ion. The research project consists of two systems: the monitoring system and the actuating system. This project accomplishes the first part and assesses the feasibility of measuring the internal impedances of batteries for low-Earth-orbit (LEO) satellites as a means to monitor battery health. It also monitors the effects caused by low temperature conditions through internal impedance measurements from 0 °C through -70 °C. It includes designing a compact system prototype having dimensions smaller than 16" x 11" x 11.75" and a total weight less than 10% of the battery weight.

I. Introduction

Low temperature environments have always posed a challenge to battery functionality in electronic systems. This is a prominent problem in space systems where environmental temperatures reach towards absolute zero. Batteries become permanently damaged if they charge or discharge at extremely low temperatures. Ideally, the monitoring process occurs while the batteries are supplying power to a load.

The first step requires developing a method to monitor battery conditions. This project explores internal impedance measurements of batteries as a solution. There exists a relationship between the temperature of the battery and its internal impedance, where the internal impedance increases as the temperature decreases [5,11,12]. With this data, protection procedures can be initiated to prevent battery damage while allowing the battery to supply to a load. Existing solutions use active heating devices to maintain operational temperature range for the batteries [5]. This project focuses on creating the system that is used to monitor the internal impedance of the battery while future groups will focus on implementing a method to prevent the batteries from freezing in low temperatures.

II. Initial Requirements and Specifications

Table 1: Initial System Requirements and Specifications

Marketing Requirements	Engineering Specifications	Justification
1, 5	Monitor the internal impedance of the battery between -70 °C to 0 °C while supplying power to a load of 1mA.	The project focuses on lower temperatures and the battery will be powering a load at low temperatures
2, 6	Keep the battery functional to a limit of -70°C while it supplying power to a load.	The lowest temperature offered by the <i>Tenney Junior</i> temperature chamber is -70 °C[13].
3	The system prototype must weigh less than 10% of the total battery weight.	System weight is defined by the battery weight since they vary depending on capacity.
7	The battery system outputs 28V±5 V[5].	This is the most common voltage rating for aircraft batteries.
5	The system prototype operates on the same battery it is monitoring.	The battery provides the main source of power for spacecraft; therefore the monitoring system must draw power from the battery that it is monitoring.
4	The total system prototype dimensions must be smaller than 16” x 11” x “11.75” [13].	Based on the internal dimensions of the <i>Tenney Junior</i> temperature chamber that is used for testing.
Marketing Requirements <ol style="list-style-type: none"> 1. Monitor battery health at low temperatures (-70°C) 2. Keep batteries functional at low temperatures (-70°C) 3. Low total weight (batteries, system) 4. Compact system 5. Powered by the same battery it monitors/controls. 6. Battery supplies power to the load while being monitored. 7. Battery output voltage is compatible to the majority of current spacecraft 		

The requirements and specifications table format derives from [1], Chapter 3.

The main customer needs for this project include having a lightweight and compact system prototype that monitors the health of the batteries and prevents them from freezing while they are supplying power to a load from temperatures of -70 °C to 0 °C. Additional customer needs include having a system that is compatible with current spacecraft systems by using a battery pack that outputs 28 V and have the monitoring system be powered by the battery pack that is being monitored. The customer needs coincide with marketing requirements in Table 1. By satisfying the marketing requirements, the customer needs are also satisfied.

The engineering specifications are determined by the advisors, initial research, and the temperature range of the temperature chamber. The first three specifications are set by the advisors of the project. First, the system must monitor the internal impedance of the battery through a temperature range of -70 °C to 0 °C while the battery supplies power to a load. This requirement is specified because in a spacecraft, the battery pack provides the main source of power. Therefore, the battery must provide power to a load without interruption. Any measurements done on the battery must not disturb the operation of the battery. Additionally, batteries are exposed to low temperatures in space. Therefore, the system must monitor the health of the battery at low temperatures.

Second, the system prototype must keep the battery functional while the battery powers a load at -70°C . as stated before, the temperature range is constricted by the temperature range of the *Tenney Junior* temperature chamber [13]. Furthermore, the battery must not become permanently damaged during operation. This specification fulfills the marketing requirement that the battery remains functional at low temperatures and that the battery supplies power at -70°C . The battery must maintain functionality because in space, batteries provide the main source of power and cannot be replaced. Therefore, the batteries must remain functional at cold temperatures.

Third, the monitoring system prototype weight must be 10% or less than the battery weight. Weight is an important factor for spacecraft. This specification allows the system prototype weight to vary with the battery it is monitoring since battery weight is a function of charge capacity and its actual weight will vary. This specification fulfills the marketing requirement of having a low overall weight. Spacecraft are weight sensitive due to fuel costs associated with launching a spacecraft[3]. Extra weight increases spacecraft launch costs. Therefore, the final system must be lightweight to reduce costs.

The fourth engineering specification is based on research done on current spacecraft specifications. Many current spacecraft operate using 28 V batteries and this specification ensures compatibility with these spacecraft [5]. This specification fulfills the marketing requirement that the battery output voltage is compatible to the majority of current spacecraft. Having compatible battery output voltages is vital because the monitoring system is designed to replace current methods of battery monitoring. Compatibility with the majority of current spacecraft allows the system to be easily implemented in current and future spacecraft.

The fifth engineering specification results from spacecraft limitations. Spacecraft have one main source of power: the battery pack. Therefore, the monitoring system prototype input power must also derive from the battery pack it monitors. This fulfills the marketing requirement of having a system powered by the same battery that it monitors.

The sixth engineering specification defines the total dimensions of the system. These dimensions are defined by the *Tenney Junior* temperature chamber. The total dimensions for the monitoring system and battery must fit within the temperature chamber in order to allow testability. This fulfills the marketing requirement of having a compact system because the test chamber size is inherently compact. Having a compact system is important because volume is an issue in spacecraft. Spacecraft have limited volume, and having a small monitoring and battery system reduces costs and allows more room for other instruments.

III. Initial Functional Decomposition (Level 0 and Level 1)

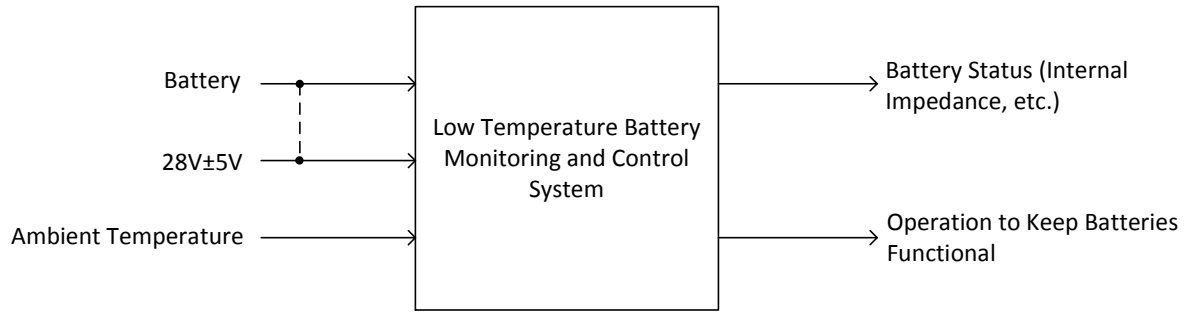


Figure 1: Initial Level 0 Block Diagram

Table 2: Initial Level 0 System Functional Requirements

Module	Low Temperature Battery Monitoring and Control System
Inputs	-Battery: The monitored battery. -28±5 V: Input power for the system prototype(from the monitored battery) -Ambient Temperature: -70 °C to 0 °C
Outputs	-Battery Status: Status of the battery (i.e. internal impedance, etc.) -Operation to Keep Batteries Functional (TBD)
Functionality	Monitor the battery's condition at low temperatures (down to -70 °C) and keep the battery functional while it is supplying to a load.

Figure 1 presents the level 0 block diagram of the low temperature battery monitoring and control system prototype. Table 2 defines the inputs, outputs, and functionality. The Battery and 28±5 V inputs are connected by a dashed line because they are the same input; the system is powered by the battery that it monitors and controls. The temperature chamber provides the ambient temperature to mimic temperatures seen in space. Since this project deals with low temperatures, the temperature range of -70 °C to 0 °C is defined. The lower temperature limit is defined by the limits of the *Tenney Junior* temperature chamber. The battery status output conveys the battery health in the form of internal impedance, etc. Lastly, our adviser instructed us to include “TBD” for our last output since this is an open-ended research project and the goal is to determine the best, if any, solution to keep the batteries functional at -70 °C while providing power to a load.

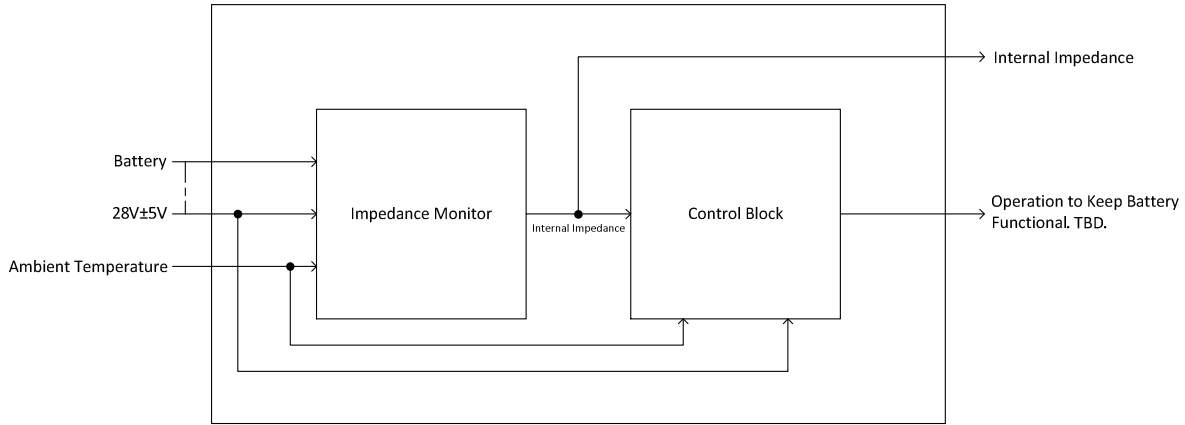


Figure 2: Initial Level 1 Block Diagram

Table 3: Level 1 Subsystem - Impedance Monitor Functional Requirements

Module	Impedance Monitor
<i>Inputs</i>	-Battery: The monitored battery. -28±5 V: Power supply for the system (from the monitored battery) -Ambient Temperature: -70 °C to 0 °C
<i>Outputs</i>	-Internal Impedance: The internal impedance of the battery
<i>Functionality</i>	Monitor the battery's condition at low temperatures (down to -70°C) and output the battery's internal impedance while it is supplying to a load.

Table 4: Level 1 Subsystem - Control Block Functional Requirements

Module	Control Block
<i>Inputs</i>	-Internal Impedance: The internal impedance of the battery -28±5 V: Power supply for the system (from the monitored battery) -Ambient Temperature: -70 °C to 0 °C
<i>Outputs</i>	-Operation to keep battery functional (TBD)
<i>Functionality</i>	Use the battery's internal impedance as an indication of health/status and executes operation to keep battery functional if necessary.

Figure 2 presents the level 1 block diagram for the LTBMCS, which is broken down into two blocks: the Impedance Monitor and the Control Block. Table 3 defines the functionality of the Impedance Monitor. The Impedance Monitor determines the battery's internal impedance while the battery supplies power to a load. The internal impedance indicates the battery's health[4,7,10]. Table 4 defines the functionality of the Control Block. The Control Block determines the battery's health based on its internal impedance and executes an operation (TBD), if necessary, to keep the battery functional.

IV. Final Requirements and Specifications

Table 5: Final System Requirements and Specifications

Marketing Requirements	Engineering Specifications	Justification
1,	Monitor the internal impedance of the battery between -70 °C to 0 °C.	The project focuses on lower temperatures.
2	The system prototype must weigh less than 10% of the total battery weight.	System weight is defined by the battery weight since they vary depending on capacity.
4, 5	The Li-ion batteries output 3.7 V \pm 0.37 V.	This is a common voltage rating of commercially available Li-ion batteries used for testing. Dr. Dolan also chose these batteries to be used for testing.
4	The system prototype uses commercially available circuit components.	The available budget limits us to commercially available circuit components for economic solutions.
3	The total system prototype dimensions must be smaller than 16" x 11" x "11.75" [13].	Based on the internal dimensions of the <i>Tenney Junior</i> temperature chamber that is used for testing.
Marketing Requirements <ol style="list-style-type: none"> 1. Monitor battery health at low temperatures (-70 °C) 2. Low total weight (batteries, system) 3. Compact system 4. Commercially available components 5. Li-ion battery technology 		

The requirements and specifications table format derives from [1], Chapter 3.

Section IV redefines the requirements and specifications for the project because the scope of the project has been reduced to the Impedance Monitor. This system is implemented to study the impedance of Li-ion batteries at low temperature. The reduction is due to the insufficient funds to purchase industrial grade components (batteries, circuit components, etc.) and insufficient time to develop both systems. Overall, the project deliverables include the Impedance Monitor and analysis of commercial Li-ion batteries based on tests conducted with the *Tenney Junior* temperature chamber. These two deliverables will allow another group to continue developing the project by implementing the Control Block.

Similar to Section II, the main customer needs for this project include having a lightweight and compact system prototype that monitors the health of the batteries from temperatures of -70°C to 0 °C. Additional customer needs include using commercially available products because they are easily accessible and our budget limits us to these components. Lastly, the battery technology under test is Li-ion as this project specifically focuses on testing Li-on batteries.

The engineering specifications are determined by the advisors, initial research, and the temperature range of the temperature chamber. In Table 5, the justifications for the first, second, and fifth specifications can be found in the initial specifications and requirements (Section II). The third engineering specification requires Li-ion batteries to output 3.7 V because this is a common voltage rating for commercially available Li-ion batteries. Furthermore, Dr. Dolan chose the specific batteries used for testing and they all have the same voltage rating with different energy rating. The fourth engineering specification requires the use of commercially available components because our available budget does not allow us to use industrial grade components. Furthermore, this will result in an economic design .

V. Final Functional Decomposition (Level 0 and Level 1)

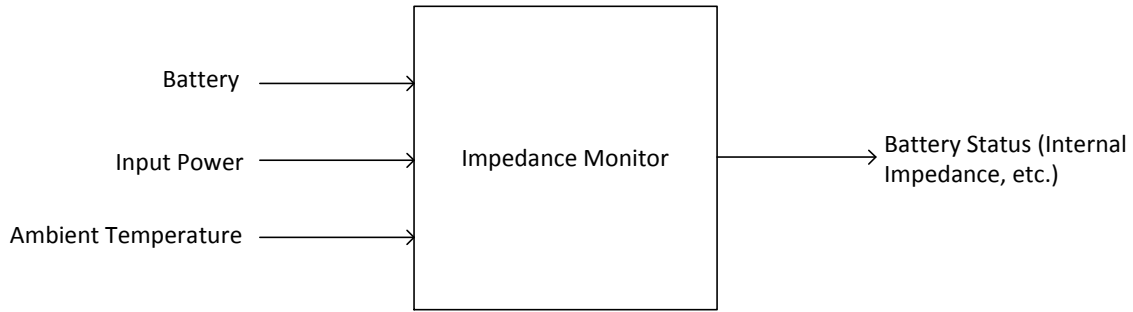


Figure 3: Final Level 0 Block Diagram

Table 6: Final Level 0 System Functional Requirements

Module	Impedance Monitor
<i>Inputs</i>	<ul style="list-style-type: none"> -Battery: The monitored battery. -Input Power: Input power for the system prototype(from the monitored battery) -Ambient Temperature: -70 °C to 0 °C
<i>Outputs</i>	-Battery Status: Status of the battery (i.e. internal impedance, etc.)
<i>Functionality</i>	Monitor the battery's condition at low temperatures (down to -70 °C)

Figure 1 presents the final level 0 block diagram of the Impedance Monitor prototype. Table 6 defines the inputs, outputs, and functionality. The temperature chamber provides the ambient temperature to mimic temperatures seen in space. Since this project deals with low temperatures, the temperature range of -70°C to 0°C is defined. The lower temperature limit is defined by the limits of the *Tenney Junior* temperature chamber. The battery status output conveys the battery health in the form of internal impedance, etc.

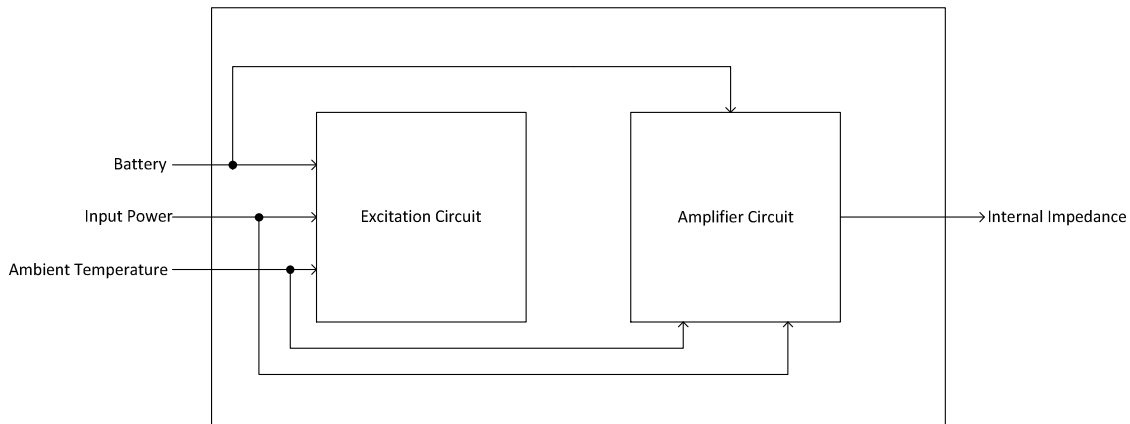


Figure 4: Final Level 1 Block Diagram

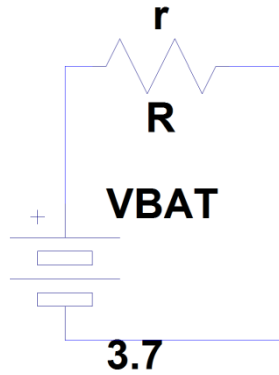
Table 7: Level 1 Subsystem – Excitation Circuit Functional Requirements

Module	Excitation Circuit
<i>Inputs</i>	-Battery: The monitored battery -Input Power: Power supply for the system (from the monitored battery) -Ambient Temperature: -70 °C to 0 °C
<i>Outputs</i>	N/A
<i>Functionality</i>	Treating the battery's internal impedance as a resistor, the excitation circuit will excite the battery by drawing current in a periodic fashion in order to create a small voltage “wiggle” proportional to the battery's internal impedance.

Table 8: Level 1 Subsystem – Amplifier Circuit Functional Requirements

Module	Amplifier Circuit
<i>Inputs</i>	-Battery: The voltage wiggle at the battery's output -Input Power: Power supply for the system (from the monitored battery) -Ambient Temperature: -70 °C to 0 °C
<i>Outputs</i>	-Output: Battery's internal impedance
<i>Functionality</i>	Amplifies the voltage wiggle proportional to the battery's internal impedance.

Figure 4 presents the level 1 block diagram for the LTBMCS, which is broken down into two blocks: the Impedance Monitor and the Control Block. Table 7 defines the functionality of the Excitation Circuit.

**Figure 5: Battery Internal Impedance Model**

As shown in Figure 5, the Excitation Circuit models the battery's internal impedance as a resistor and produces a voltage wiggle proportional to the internal impedance by drawing current in a periodic fashion. The internal impedance indicates the battery's health [4,7,10]. Table 8 defines the functionality of the Amplifier Circuit. The Amplifier Circuit amplifies the voltage wiggle so that the internal impedance can be visually observed on an oscilloscope.

VI. Internal Impedance Monitor Design

A battery's internal impedance will ideally be very small, similar to an ideal DC voltage source. Therefore, the resulting proportional voltage will be very small and will be buried in noise. A variant of the lock-in amplifier was chosen because it can extract small input signals buried in noise by generating a DC voltage proportional to small input signals buried in noise.

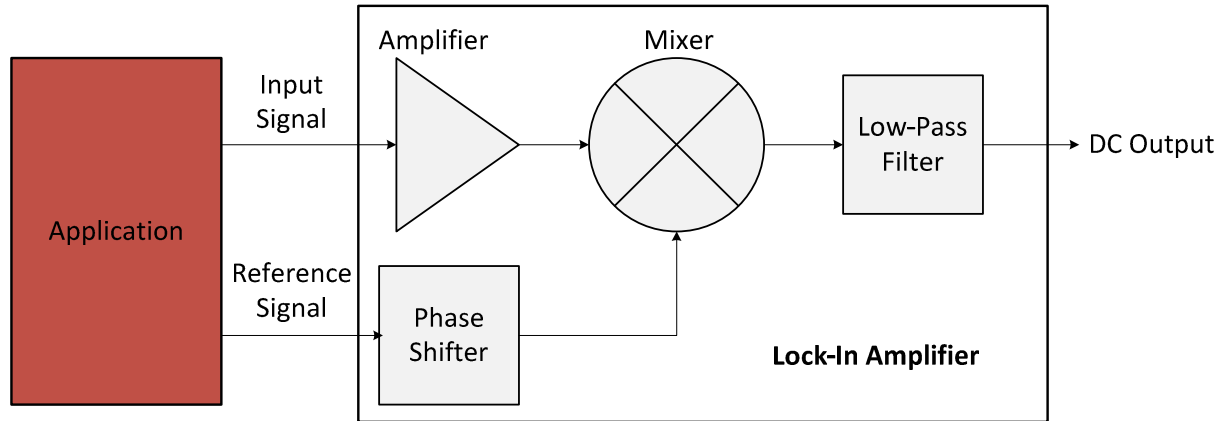


Figure 6: Generic Lock-In Amplifier Schematic

As shown in Figure 6, a generic lock-in amplifier consists of an amplifier, a mixer, and a low-pass filter (the phase shifter is optional). It requires both the input signal and a reference signal with the same frequency as the input signal from the application. For our application, the excitation circuit produces both the input signal and reference signal. The small input signal is amplified and mixed with the reference signal, generating a new signal that includes a DC component proportional to the input signal. This can be understood if we considering multiplying two sine functions of the same frequency together, resulting in a new function consisting of a DC component and another sine function with twice the original frequency. The DC component is then extracted using a low-pass filter. The phase shifter is included just in case the reference signal needs to be phase shifted to be in phase with the amplified input signal.

The frequency of 1 kHz is chosen for this design because this circuit would ideally be monitoring a battery that is supplying to a load and low frequency operation would affect the battery the least because it generates a slower varying ripple at the battery's output.

A. Excitation Circuit

i. Design

A series LC circuit was originally considered as the excitation circuit because these passive components ideally do not dissipate power.

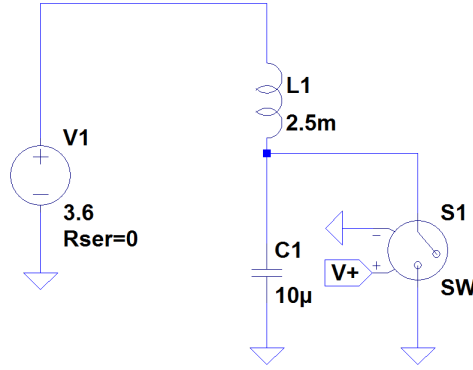


Figure 7: Initial Excitation Circuit - LC Circuit

The resonant frequency of the LC circuit is defined as

$$f_o = \frac{1}{2\pi\sqrt{LC}} \quad (1)$$

The component values are chosen by setting (1) equal to 1 kHz. The switch is initially closed to charge the inductor. When the switch opens, the inductor charges the capacitor. Through resonant operation, the LC circuit effectively draws sinusoidal current and creates a voltage wiggle proportional to the battery's internal impedance to appear at the battery's input terminal. It is also important to note that in modeling the battery's internal impedance as a series resistor, the internal impedance will cause damping and the inductor will have to be periodically charged by the switch using a specific control scheme.

However, as shown in Figure 7, designing this circuit for a resonant frequency of 1 kHz requires large component values. In reality, since the inductor cannot be too large, the capacitor must be larger to achieve the same frequency. Discharging this large capacitor at a fast rate requires a large current that we cannot provide. Thus, this circuit is not practical in terms of circuit component values.

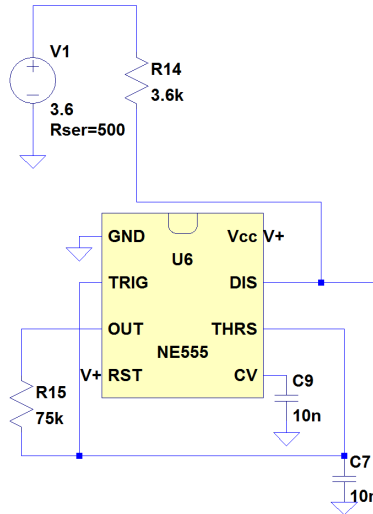


Figure 8: Final Excitation Circuit - 555 Timer Circuit

Abandoning the reactive approach, the 555 timer configuration shown in Figure 8 was considered as the next possible excitation circuit.

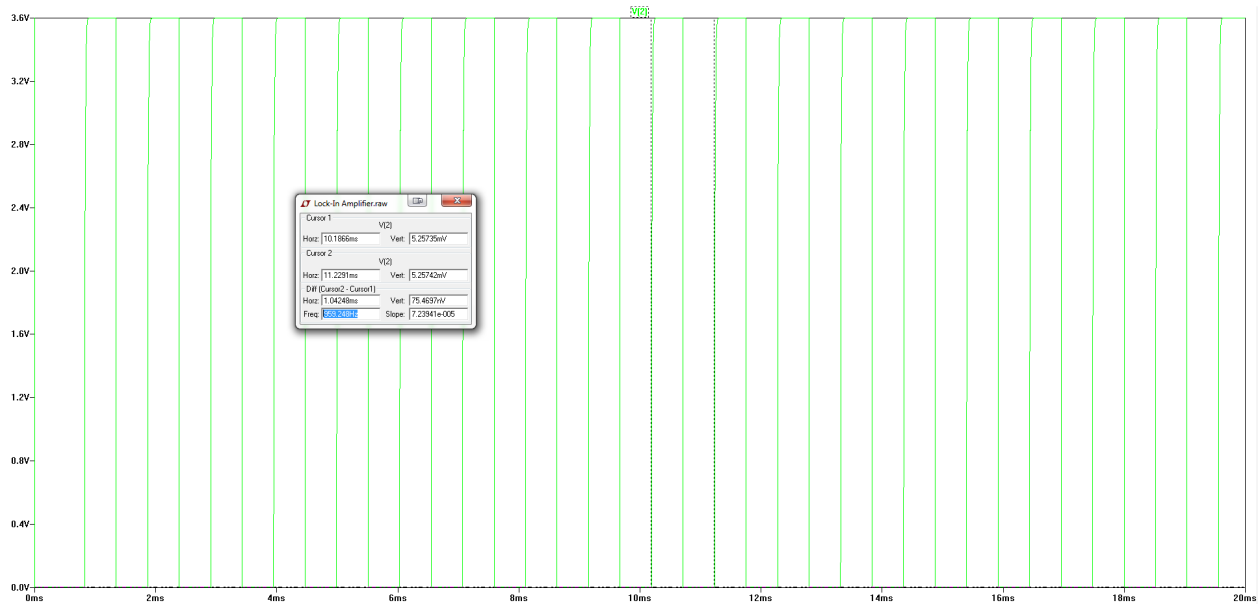


Figure 9: 555 Timer Circuit Transient Simulation

The 555 timer configuration produces both the input and reference signals by turning on/off the open-collector BJT at the DIS pin, pulling $\sim 1\text{mA}$ from the battery through the $3.6\text{ k}\Omega$ resistor and effectively producing square waves at 960 Hz from $\sim 0\text{V}$ to $\sim 3.6\text{ V}$ (refer to Figure 9). The 3.6 V serves as an indication of the battery output voltage. This operation causes a small voltage wiggle ($<1\text{ mV}$) from the battery that serves as the input signal. The square waves also serve as the reference signal for the mixer via the MOSFET.

Phase shifting circuitry is not necessary for this implementation of the lock-in amplifier because square waves are used for excitation.

ii. Testing

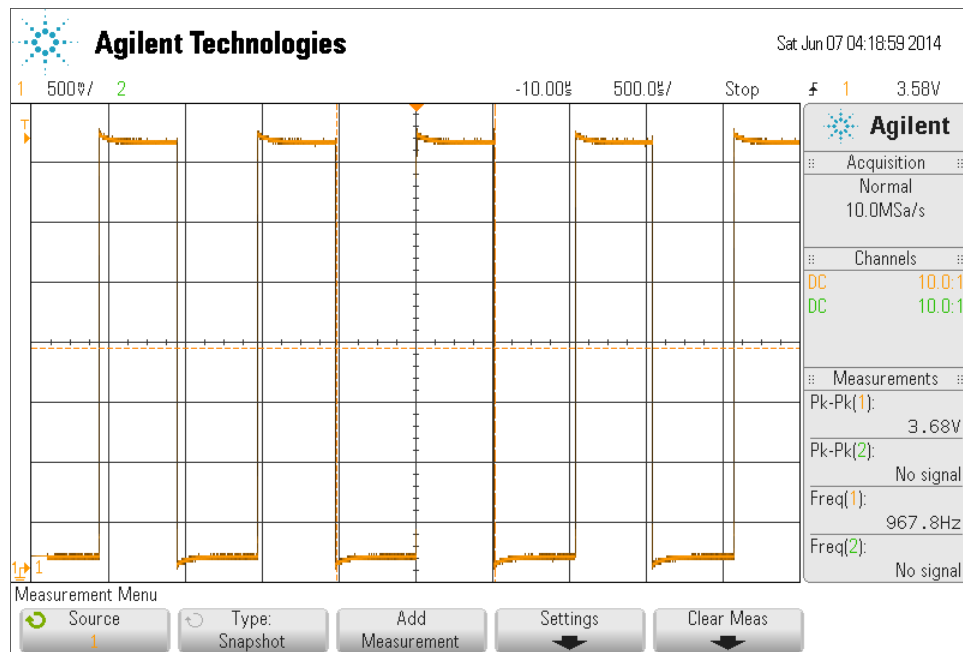


Figure 10: 555 Timer Circuit Experimental DIS Waveform

Figure 10 presents a scope capture of the DIS pin on the 555 Timer circuit. As shown, the DIS pin sinks current at 967.8 Hz, which matches the simulation shown in Figure 9 and confirms correct operation.

B. Amplifier Circuit

i. Design

The amplifier chain consists of three parts: the amplifier, the mixer, and the low-pass filter.

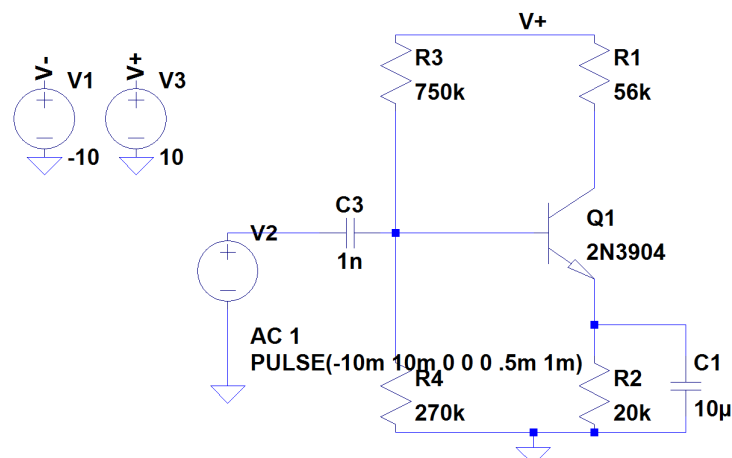


Figure 11: Discrete Amplifier Schematic

The amplifier is made using discrete components. The input AC coupling capacitor and bias resistors effectively serve as a high-pass filter and were chosen such that the cut-off frequency is ~1 kHz and 100

μA flows through the common-emitter gain stage. The $10\ \mu\text{F}$ bypass capacitor boosts the gain by effectively shorting the $20\ \text{k}\Omega$ resistor at the frequency of operation. The $56\ \text{k}\Omega$ resistor helps set the output DC voltage and the gain to allow enough room for voltage swing.

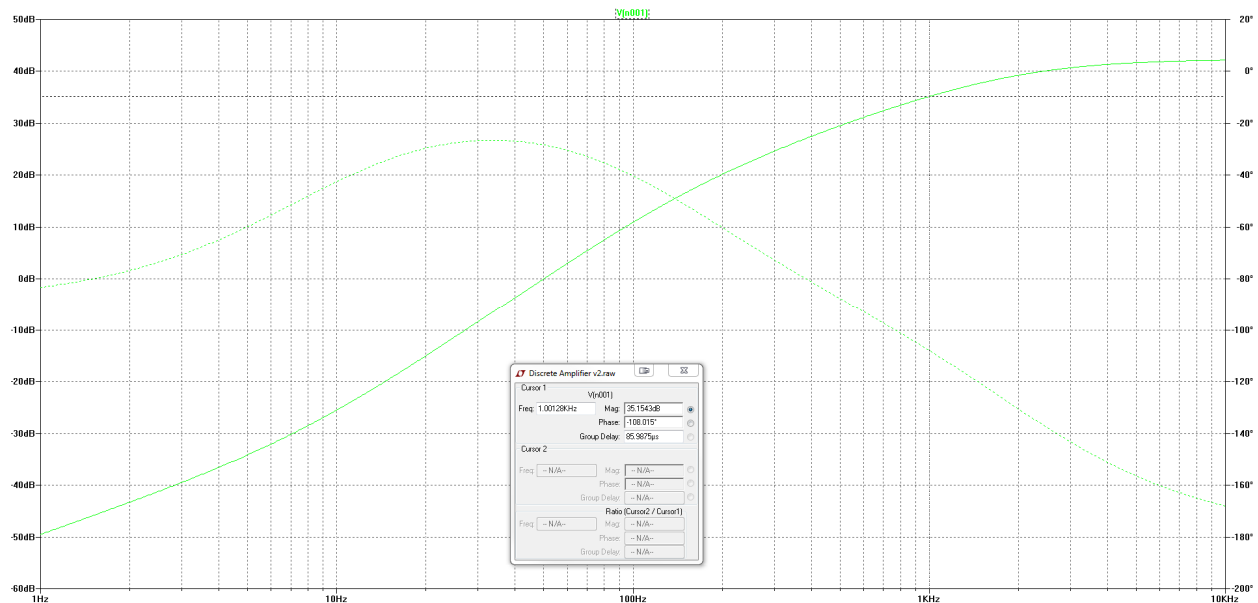


Figure 12: Frequency Response of Discrete Amplifier

The gain is $\sim 35\ \text{dB}$ at $1\ \text{kHz}$, as shown in Figure 12.

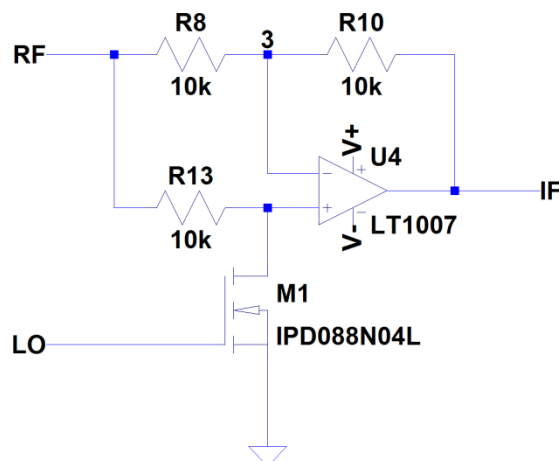


Figure 13: Chopping Mixer Schematic

A chopping mixer is implemented using an op-amp with three well-matched $10\ \text{k}\Omega$ resistors. The reference signal from the 555 timer configuration acts as the LO signal and drives the MOSFET used to "chop" the signal, effectively multiplying the waveform by "1" and "-1" at a frequency of $1\ \text{kHz}$. This operation can be seen with the following analysis: when the MOSFET is off, the input voltage appears at both input terminals of the op-amp reflects to the output (input waveform is multiplied by "1"). When the

MOSFET is on, the non-inverting terminal of the op-amp is grounded and the entire circuit effectively becomes an inverting buffer (input waveform is multiplied by “-1”).

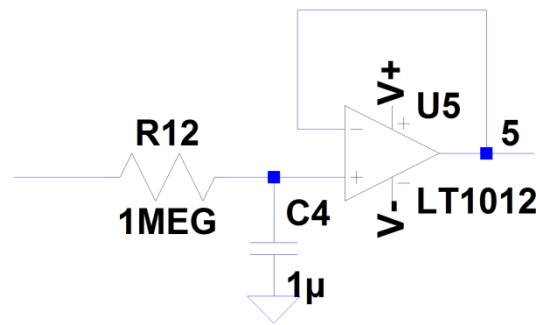


Figure 14: Buffered Low-Pass Filter Schematic

The low-pass filter used to extract the DC output is implemented using a $1\text{M}\Omega$ resistor and a $1\mu\text{F}$ capacitor with a cut-off frequency of $f_{-3\text{dB}} = \frac{1}{2\pi RC} = \frac{1}{2\pi(1\text{MHz})(1\mu\text{F})} = 0.159\text{ Hz}$.

The voltage follower at the end is used to buffer the output to prevent loading the low-pass filter.

ii. Testing

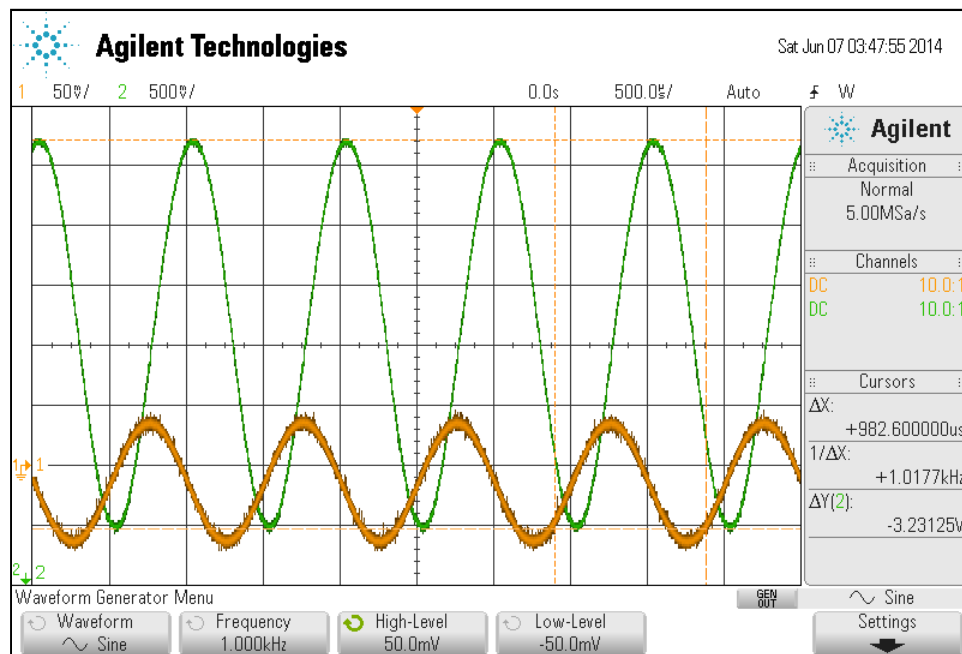


Figure 15: Discrete Amplifier Gain @ 1 kHz; green = output, yellow = input

Figure 15 shows a gain of $20 \log \left(\frac{3.23125}{0.100} \right) = 30.187\text{ dB}$. Although slightly less than the simulated gain of 35 dB, this discrete amplifier still provides the gain needed to amplify the voltage wiggle (in the microvolt range).

The chopping mixer and buffered low-pass filter components were not test separately for functionality.

C. Completed Design

i. Design

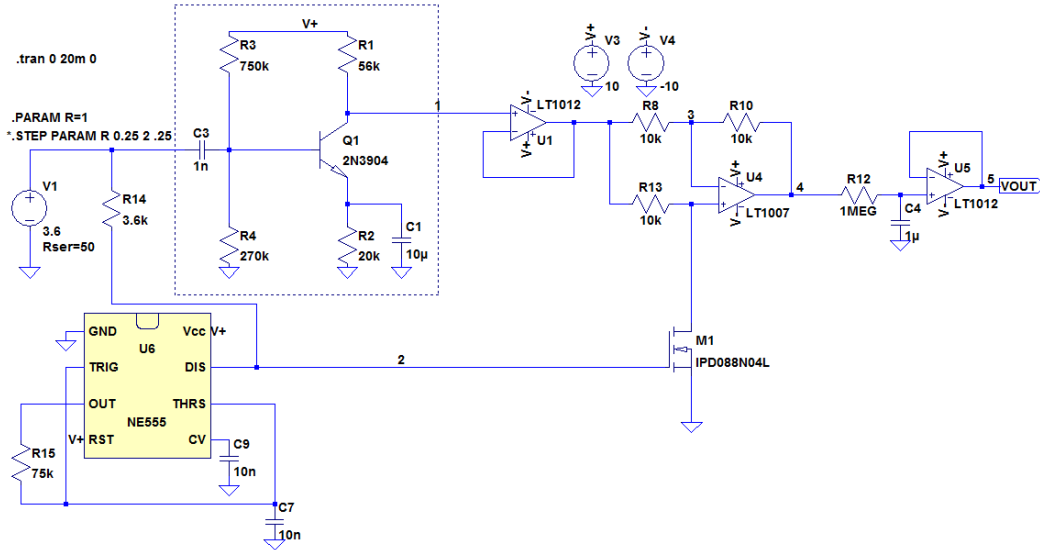


Figure 16: Complete Lock-In Amplifier Design for Battery Internal Impedance Measurements

Figure 16 presents our complete implementation of the lock-in amplifier used to monitor the internal impedance of the battery. The voltage source V1 is used to emulate a battery with an internal resistance. This simulation models the internal impedance of the battery as a resistor. The 555 Timer circuit excites the battery and creates a voltage wiggle. The discrete amplifier amplifies the voltage wiggle. The amplified voltage wiggle is mixed with another signal of the same frequency, producing a DC component proportional to the input signal and another signal with twice the original frequency. The DC component is extracted via the low-pass filter and is buffered for monitoring.

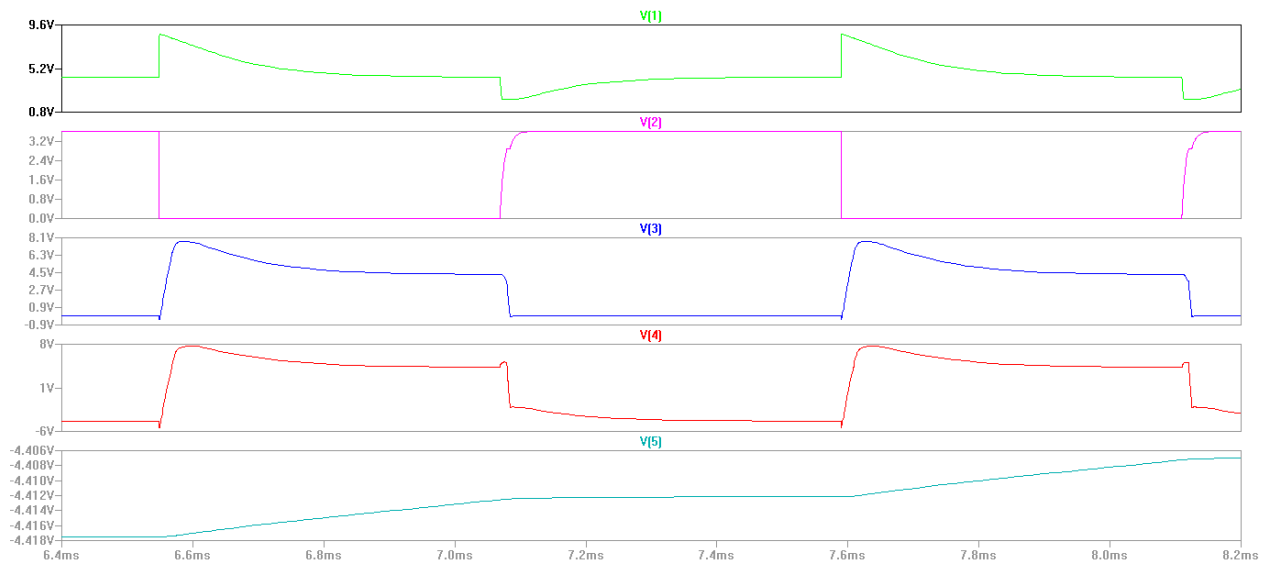


Figure 17: Lock-In Amplifier Transient Simulation - Key Waveforms

Figure 17 shows key waveforms as labeled on the schematic shown in Figure 16. V(1) shows the output of the discrete amplifier and confirms its operation with its amplified "high-passed" characteristics. V(2) shows the waveform used to excite the battery through the 3.6 k Ω resistor and drive the LO port of the chopping mixer. V(3) shows the waveform at the inverting terminal of the chopping mixer op-amp. V(4) shows the output of the chopping mixer and confirms the operation of the chopping mixer based on previous observations. Lastly, V(5) shows the DC output of the lock-in amplifier.

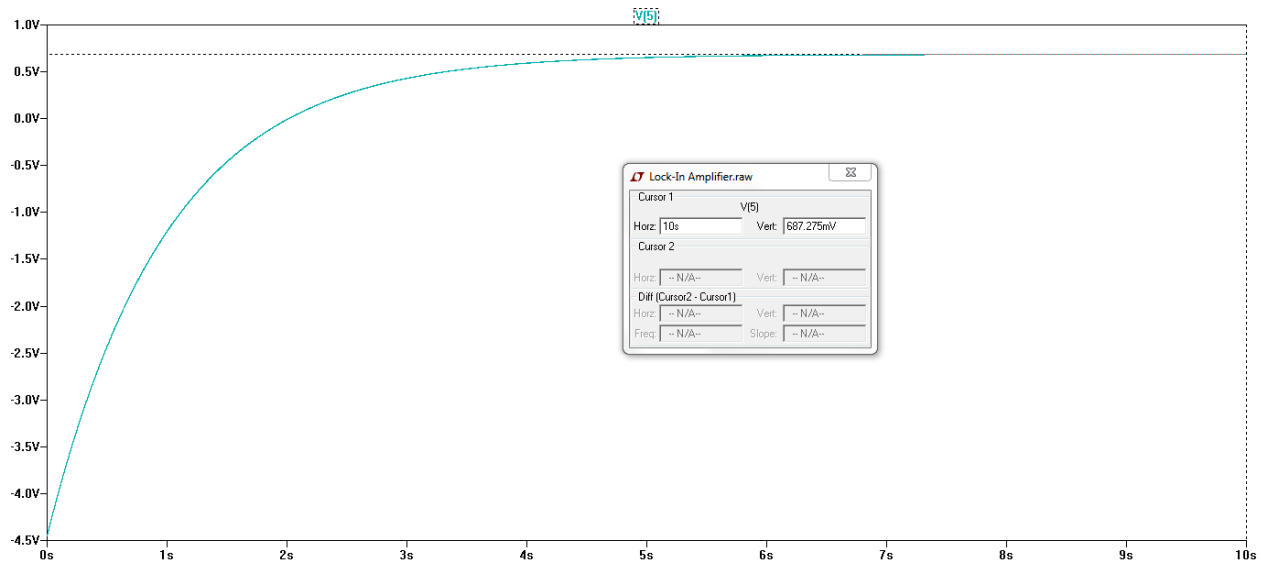


Figure 18: Lock-In Amplifier Steady-State DC Output Simulation

Figure 18 shows the steady-state DC output after running a transient simulation for 10 seconds. As shown, the steady-state output is about 687 mV.

Looking at the DC output voltage, one can already see that the DC output voltage will not be useful as a proportional measurement of the internal impedance. Instead, the DC output voltage will be useful as a direct indication of dramatic changes in internal impedance.

ii. Testing

A potentiometer is included to emulate the internal resistance of the lock-in amplifier. The following scope captures are taken at labeled nodes shown in Figure 16 for potentiometer values of $28.8\ \Omega$ and $103\ \Omega$, and confirm the operation of the lock-in amplifier by showing that the output DC voltage increases with increasing resistance.

For $r_{in} = 28.8\ \Omega$:

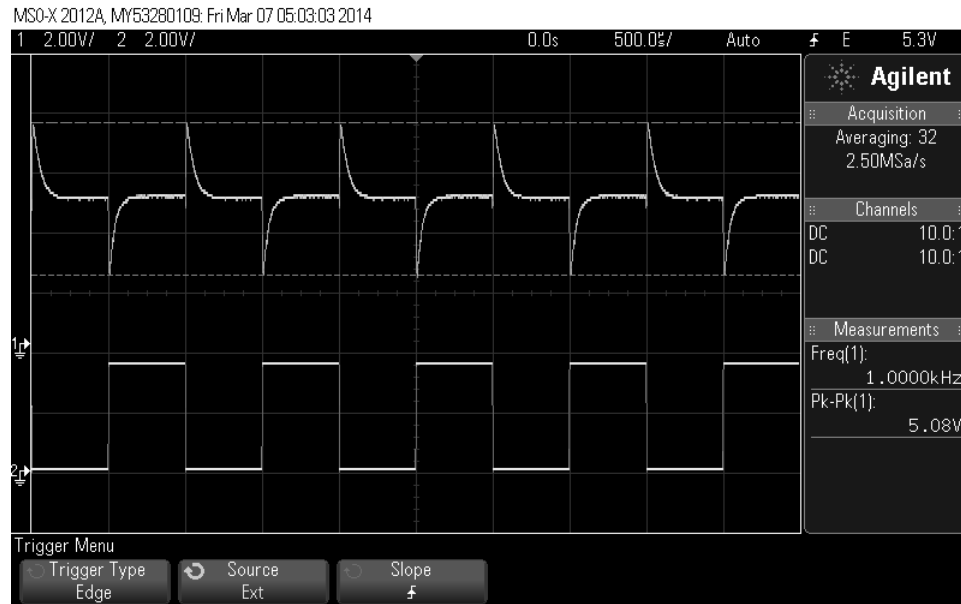


Figure 19: $r_{in} = 28.8\ \Omega$ – Ch.1 = Output of Discrete Amplifier; Ch.2 = 555 Timer DIS Pin

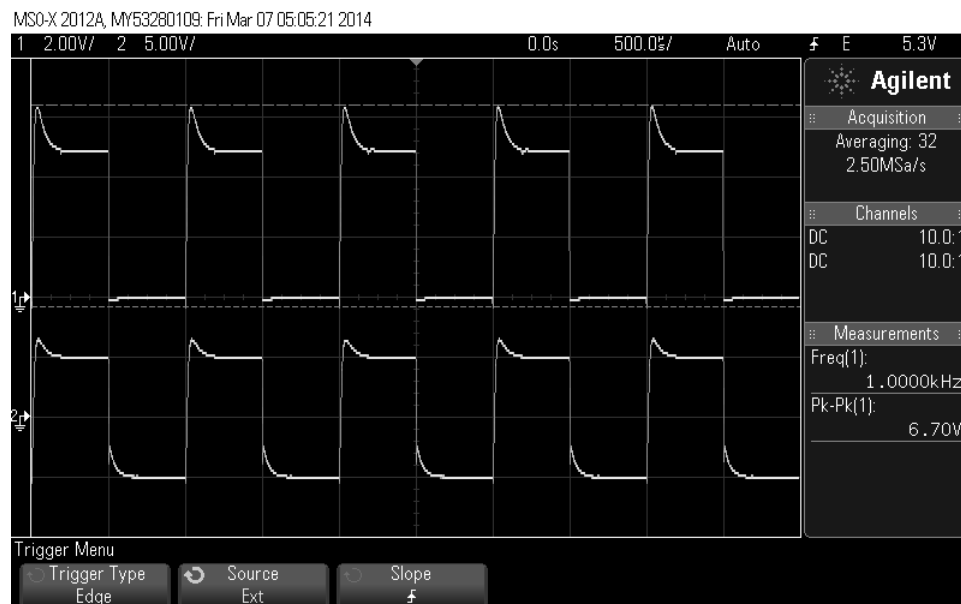


Figure 20: $r_{in} = 28.8\ \Omega$ – Ch.1 = Drain of MOSFET for Chopping Mixer; Ch.2 = Output of Chopping Mixer

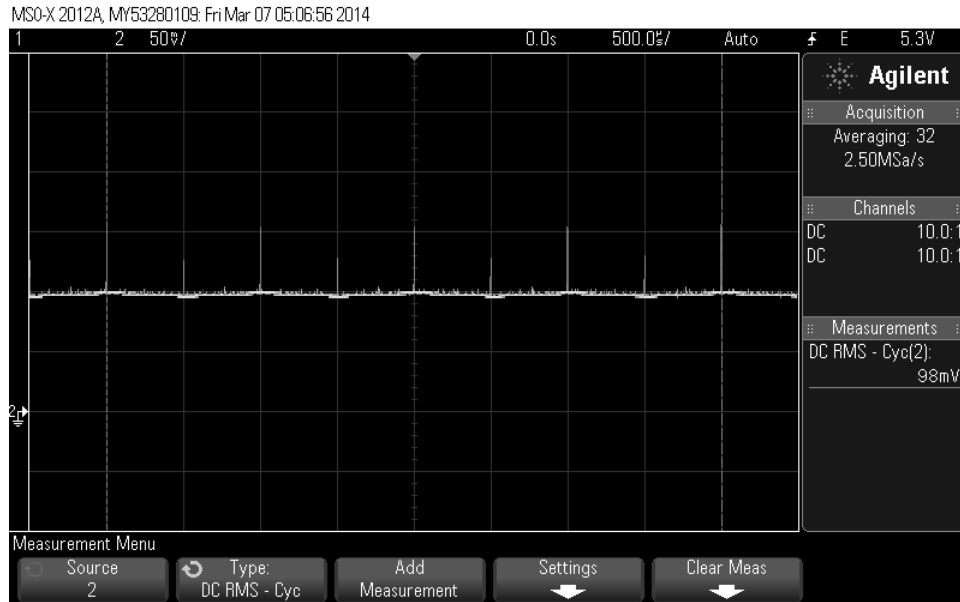


Figure 21: $r_{in} = 28.8 \Omega$ – Output DC Voltage of Lock-In Amplifier

For $r_{in} = 103 \Omega$:

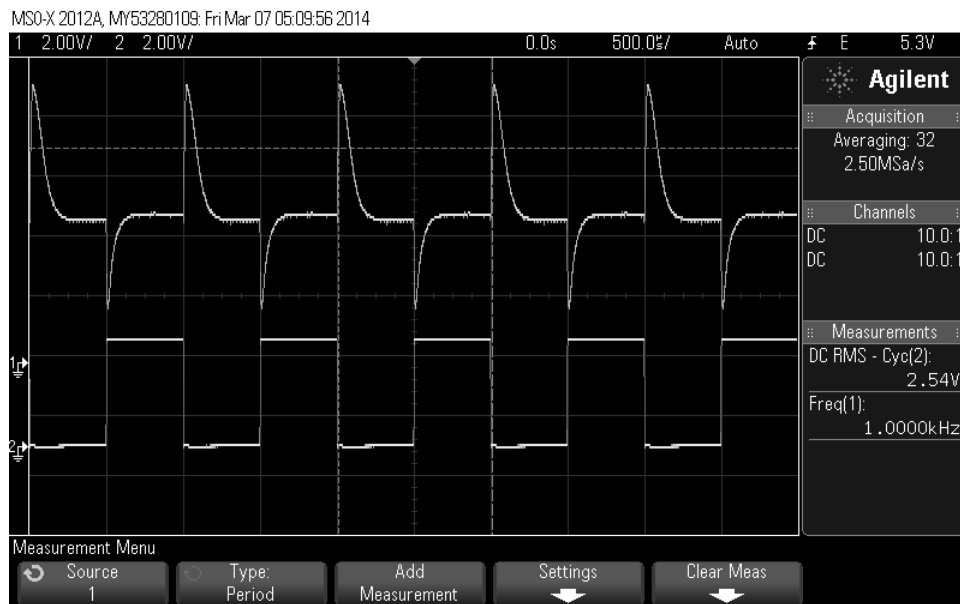


Figure 22: $r_{in} = 103 \Omega$ – Ch.1 = Output of Discrete Amplifier; Ch.2 = 555 Timer DIS Pin

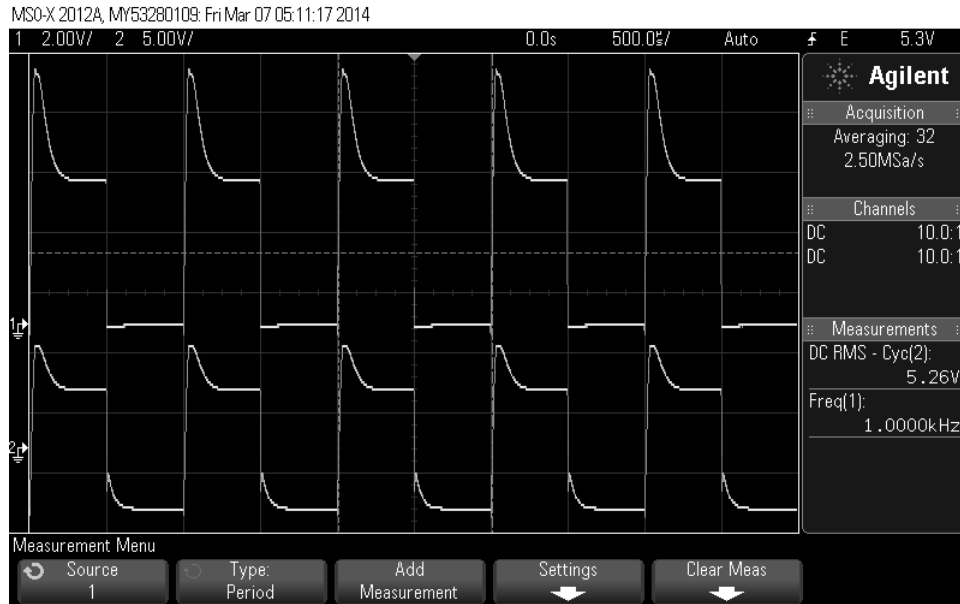


Figure 23: $r_{in} = 103 \Omega$ – Ch.1 = Drain of MOSFET for Chopping Mixer; Ch.2 = Output of Chopping Mixer

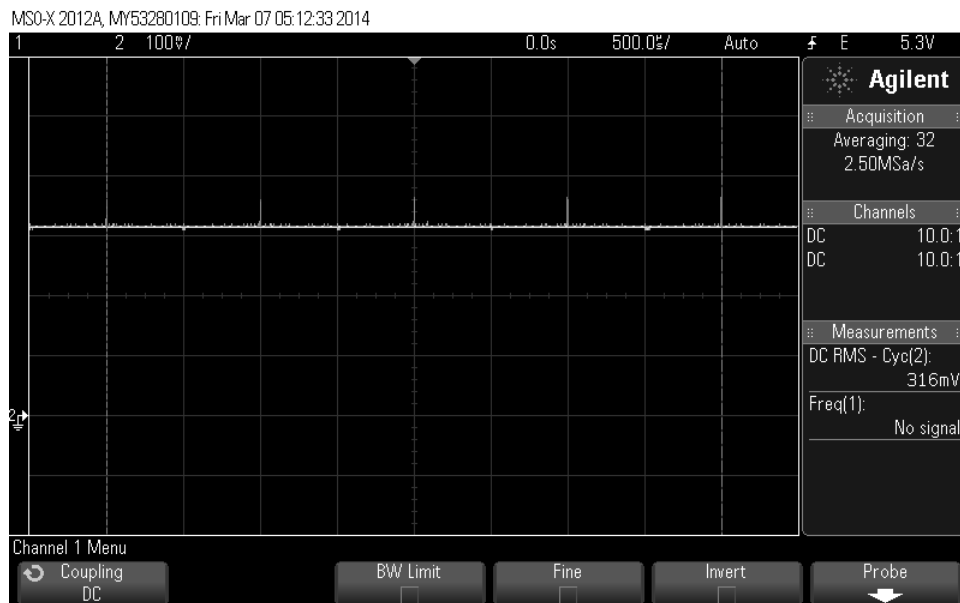


Figure 24: $r_{in} = 103 \Omega$ – Output DC Voltage of Lock-In Amplifier

The chopping mixer operation can be confirmed by comparing Ch.1 of Figure 19 and Ch.2 of Figure 20 (or Ch.1 of Figure 22 and Ch.2. of Figure 23), where the output of the chopping mixer keeps the positive portion of the amplified input signal and inverts the negative portion of the amplified input signal.

The operation of the battery internal impedance monitor can be confirmed by noting the increase in output DC voltage from 98mV (Figure 21) to 316mV (Figure 24) for an increase in resistance from 28.8Ω to 103Ω .

VII. Internal Impedance Monitor PCB

A. Design

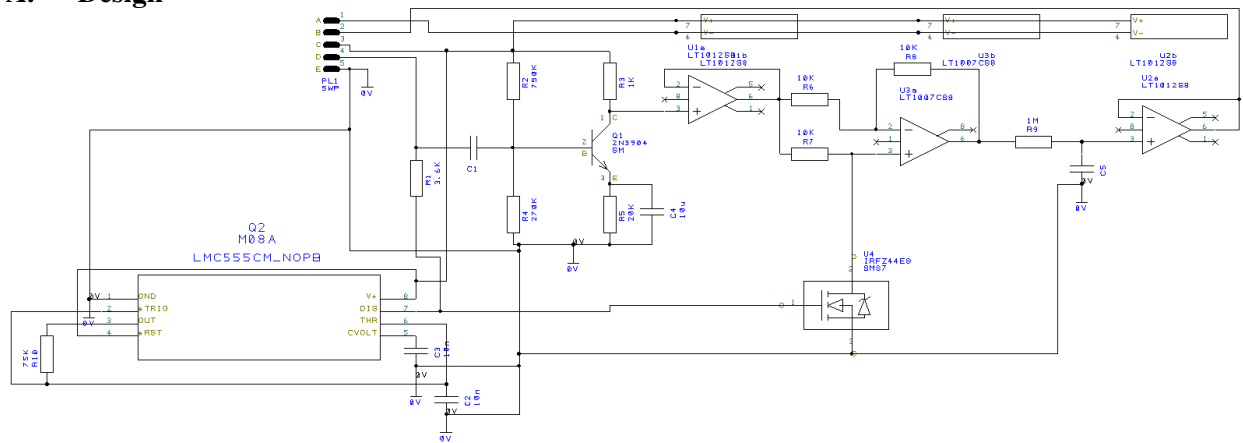


Figure 25: Impedance Monitor PCB Artist Schematic

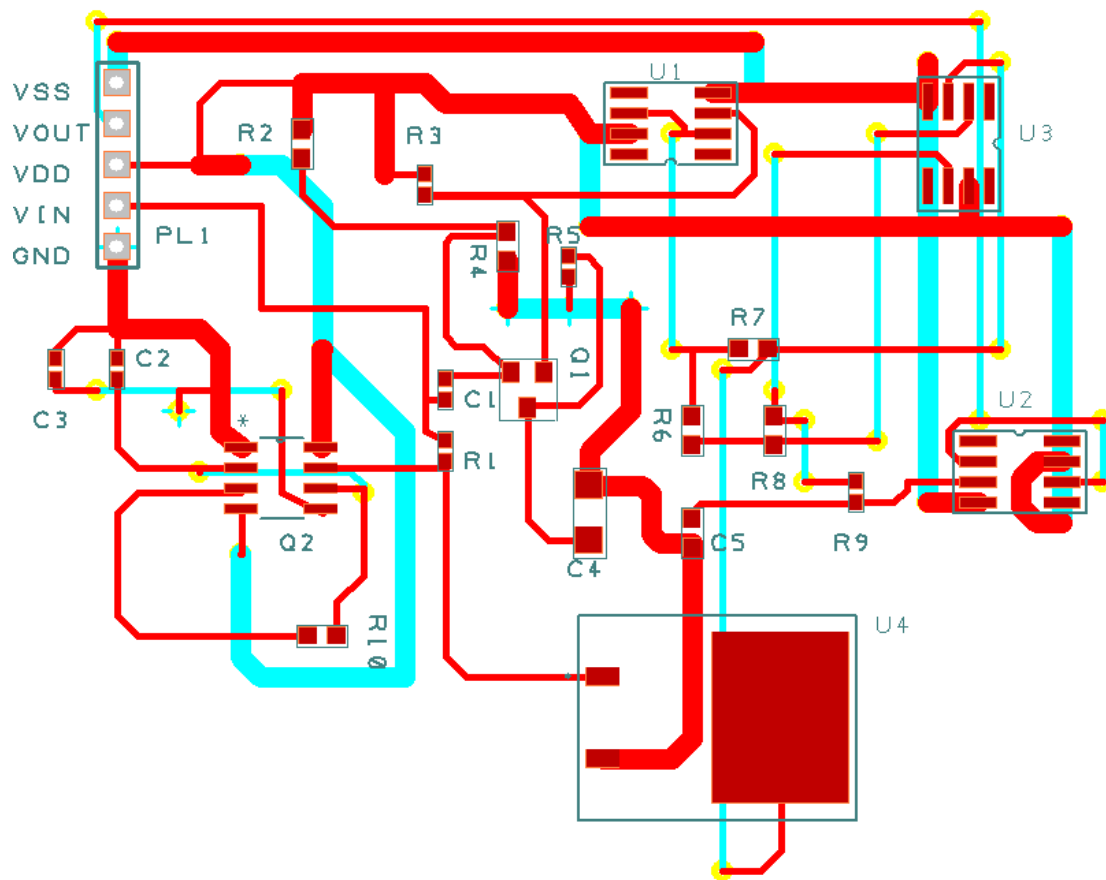


Figure 26: Impedance Monitor PCB Layout

A PCB is designed to minimize the physical size of the monitor in addition to having a system that is physically stable. The main difference between the prototype and the PCB is the use of surface mount components for the PCB.

Some research was conducted on the durability of FR4 PCB's at low temperatures, but little information is available on the durability of FR4 at low temperatures. One study shows that small cracks can appear in FR4 at low temperatures [14]. Due to the low cost of FR4 and the budget restraint of this project, an FR4 PCB was designed.

B. Testing

The PCB was first used to monitor the impedance of a known battery at room temperature. After verifying the key waveforms, a battery temperature sweep impedance test was conducted to confirm the accuracy of the measurements.

C. PCB Freeze Test

Purpose:

The purpose of the PCB freeze test is to show the performance of the lock-in amplifier under the stress of temperature. The battery would not be the only component under the effects of low temperature, so a PCB with all discrete components for the lock-in amplifier must be tested. If the PCB does fail, the temperature at which it fails will be recorded. This information will determine whether or not temperature protection will be needed for the lock-in amplifier in future designs of the battery monitoring system.

Procedure:

The lock-in amplifier PCB is placed inside the temperature chamber while the battery it is measuring remains outside of the chamber. This isolation is necessary to see the effects of temperature on the PCB alone. The temperature chamber is set to sweep in a temperature range of 25 °C to -70 °C, the same temperature sweep range for the battery impedance and temperature sweep tests. The output voltage of the lock-in amplifier and the voltage at the gate of the MOSFET are measured with an oscilloscope. Observing the gate of the MOSFET will determine whether or not the chopping mixer is still functional if the entire lock-in fails. If the PCB does fail, the output voltage will be a large value, around the range of 4.7 V and 4.8 V. The temperature at which the lock-in fails is recorded and the operation of the chopping mixer is checked.

Results:

Figure 27 shows the PCB temperature sweep test results, with the data beginning at 22.3 °C and terminating at -20.7 °C. The output DC voltage of the lock-in increases steadily as the temperature of the PCB decreases. The lock-in ceases to function at -20.7 °C, with the output voltage recorded as 4.71 V, and is the final data point to be recorded. At this temperature, the lock-in has failed due to the 555 timer no longer oscillating. Industrial or military grade discrete components would be necessary in order to withstand the low temperatures, as commercial grade components are not suited for such low temperatures.

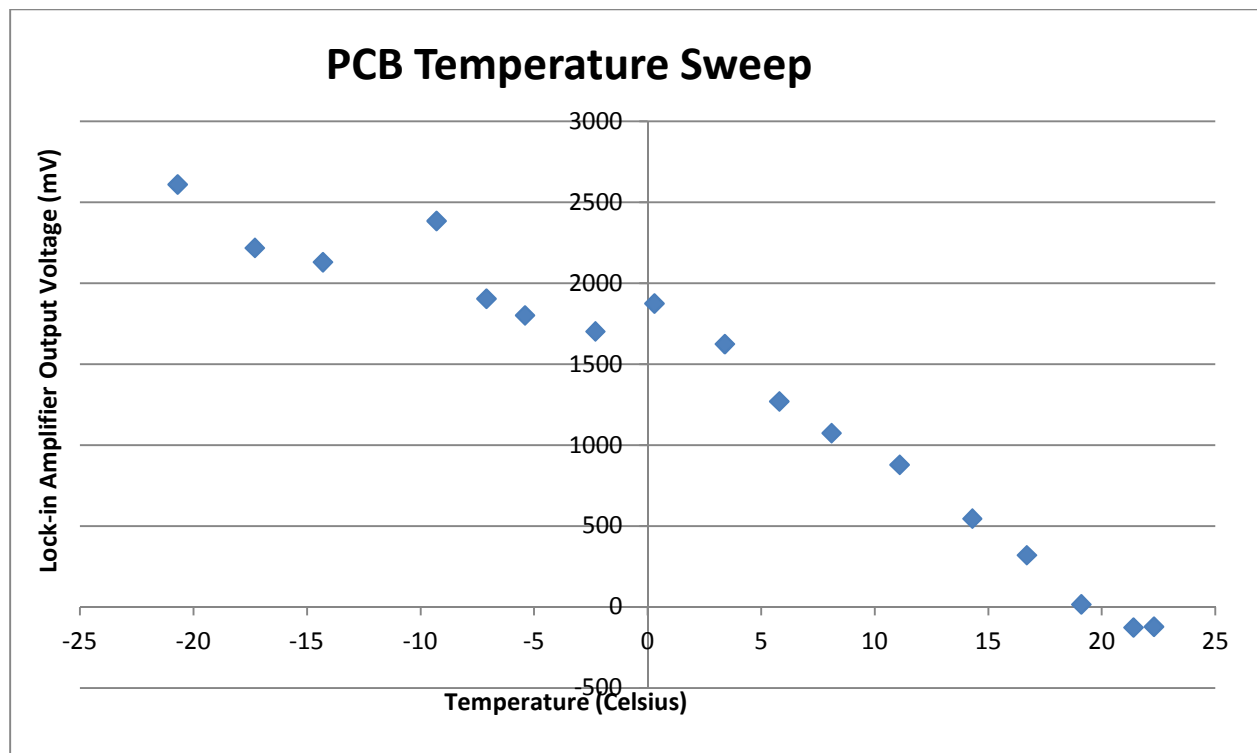


Figure 27: PCB Temperature Sweep Test Results

VIII. Lithium-Ion Battery Tests

A. Room Temperature Impedance Characterization Tests

Purpose:

Before any impedance measurements at low temperatures can be made on any batteries, the lock-in amplifier had to be characterized in terms of the oscillation frequency of the chopping mixer and output voltage. These characterizations are performed with both 3400 mAh and 3100 mAh rated lithium-ion batteries (A-Type and B-Type respectively) at approximately 21°C (room temperature). By finding the relationship between the mixer frequency and the output voltage, a chosen frequency can be determined for the lock-in amplifier when running other tests. For the lock-in amplifier, the base frequency of the 555 timer is chosen to be around 1 kHz and frequencies around that value are tested.

Procedure:

The lock-in amplifier is set up to measure the impedance of both the A-Type and B-Type batteries at room temperature (specified at ~21 °C). The frequency that the 555 timer oscillates is varied between 900, 1000, and 1100 Hz when measuring a single battery. The output voltage is recorded at each frequency for each battery. In this experiment, 8 A-Type batteries and 10 B-Type batteries are used to find an average lock-in output voltage at each frequency.

Results:

Figure 28 shows that as the frequency of the chopping mixer increases, the output DC voltage of the lock-in amplifier decreases. Table 9 shows the average output voltages at each frequency for each battery. On average, changing the frequency by 100 Hz changes the output voltage by approximately 0.01 V. It was determined that 1 kHz would stay as the frequency for which the 555 timer would oscillate at, since it is a distinct frequency that is not too high or too low and it establishes a measurable output voltage.

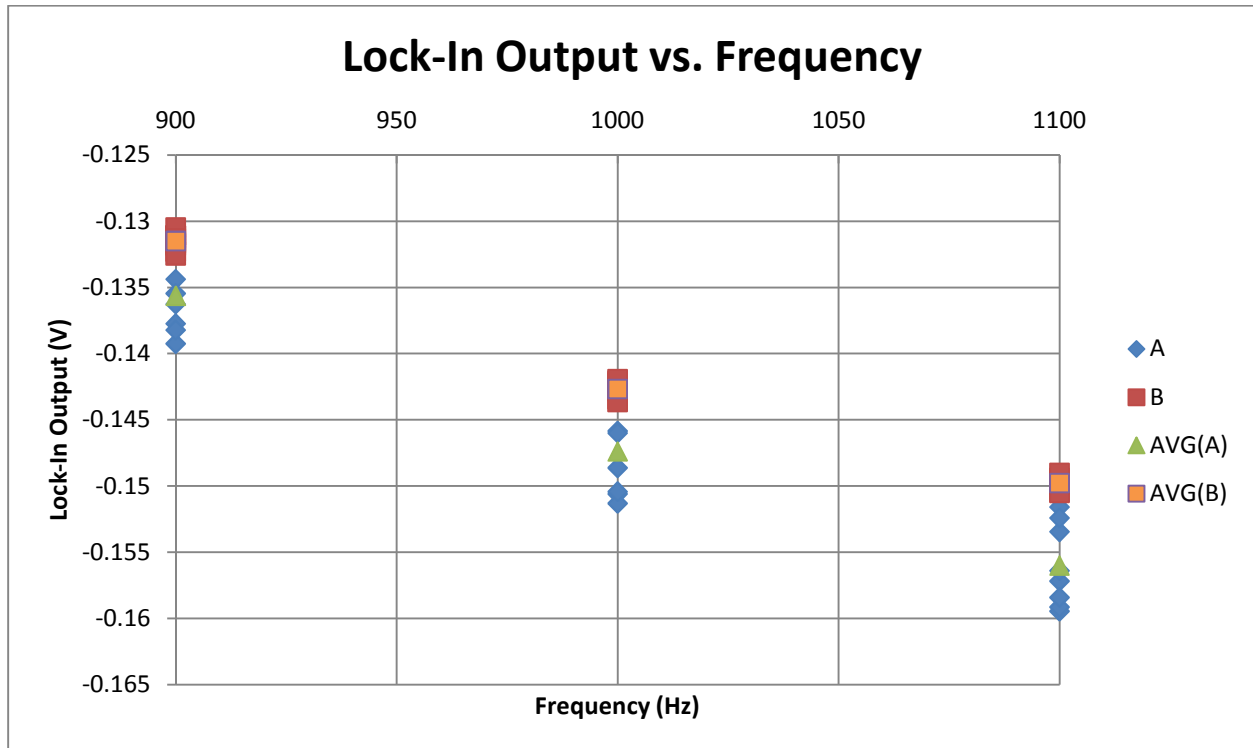


Figure 28: Lock-in Output vs. Frequency of Batteries at Room Temperature

Table 9: Average Output Voltages of Lock-In Amplifier at Varying Chopping Mixer Frequencies

Chopping Mixer Frequency (Hz)	A-Type Average Output Voltage (V)	B-Type Average Output Voltage (V)
900	-0.1356	-0.1314
1000	-0.1474	-0.1427
1100	-0.1560	-0.1498

B. Temperature Sweep Impedance Sweep Tests

Purpose:

The purpose of the internal impedance and temperature sweep test is to define a relationship between the temperature of the battery and the output voltage the lock-in amplifier. This information will establish the failure point of the battery by defining the temperature and associated impedance at which the battery breaks. This data can be used when designing the control system that prevents the batteries from incurring damage during its failure point.

Procedure:

For the temperature sweep tests, 3400 mAh and 3100 mAh rated lithium-ion batteries are used and are classified as A-Type and B-Type batteries respectively. The lock-in amplifier is used to measure the internal impedance of the test batteries and is represented with an output DC voltage. The batteries are placed in the temperature chamber and isolated from the lock-in amplifier. An oscilloscope is used to measure the average output DC voltage of the lock-in amplifier as well as the output signal of the discrete amplifier within the lock-in amplifier. Observing the discrete amplifier output verifies the operation of the lock-in amplifier. The temperature chamber sweeps through a temperature range of 25 °C to -75 °C through a 2 hour test period. This amount of time is necessary to allow the battery to reach an equilibrium temperature with the temperature chamber. The output DC voltage from the lock-in is recorded every 5 minutes or approximately every decrease in temperature by 4 °C.

Results:

Two A-Type and B-Type batteries go through two iterations of the temperature sweep test. Figure 29, Figure 30, Figure 31, and Figure 32s how the results of the impedance vs. temperature tests for both battery types. A trend is observed between both battery types across all tests, where the impedance measurements increase steadily from -40 °C to -55 °C approximately. Afterwards, the impedance measurements increase rapidly between -55 °C and -60 °C in a short period of time before reaching a terminal ~4.8 V.

The 4.8 V saturation can be justified by the output of the discrete amplifier clipping at the rails. The voltage wiggle increases as the internal impedance increases and will eventually cause the output of the discrete amplifier to clip at the rails, resulting in the same DC output voltage, regardless of the change in internal impedance. This is not a problem for our application because the purpose is to determine the point at which the battery is on the verge of freezing and the drastic changes show that.

For the A-Type batteries, the first and second freeze tests for A5 and A7 do not show any significant differences in terms of data. Both tests and their iterations of freeze tests show the same trend of a steady increase in impedance between -45 °C and -55 °C, a rapid increase in impedance from -55 °C to -60 °C approximately, and terminating at ~4.8 V. B-Type batteries B5 and B9 show a similar trend of increase, but at different temperatures. Figure 31 shows the increase in impedance for B5 occurring at -55 °C in the second freeze attempt when the increase occurred at -45 °C in the first freeze attempt. Figure 32 shows the

reverse, where the increase in impedance for B9 occurs at -47 °C in the second freeze attempt when the increase occurred at -55 °C in the first freeze attempt.

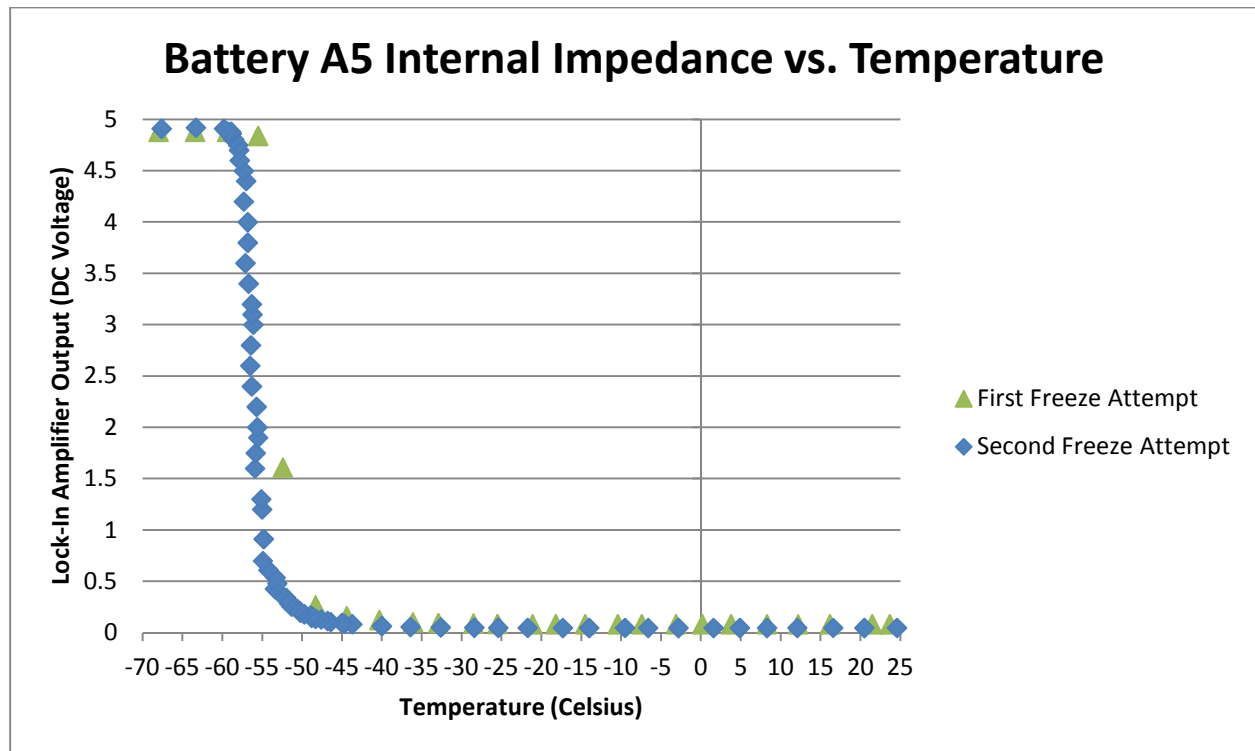


Figure 29: A5 Impedance vs. Temperature Test Results

The results from the B-Type and A-Type support two observations. The first is that the internal impedance of a battery will have a steady increase in impedance before having a rapid increase in impedance at a certain temperature. The other observation is that multiple freeze attempts do not affect subsequent temperature tests and is due to the internal protection circuitry in the lithium-ion batteries. A possible explanation for the variation in the B-Type tests is that the batteries may not have been fully charged when the tests were conducted. This could lead to the impedance increasing at different temperatures.

An important area to observe in all sets of data is the region of a steady increase in impedance before it rapidly increases. Continuous use of a battery and damage prevention is possible if the temperature of the battery is controlled. Specifically, regulation of battery temperature can be performed at a specific temperature rather than having constant regulation.

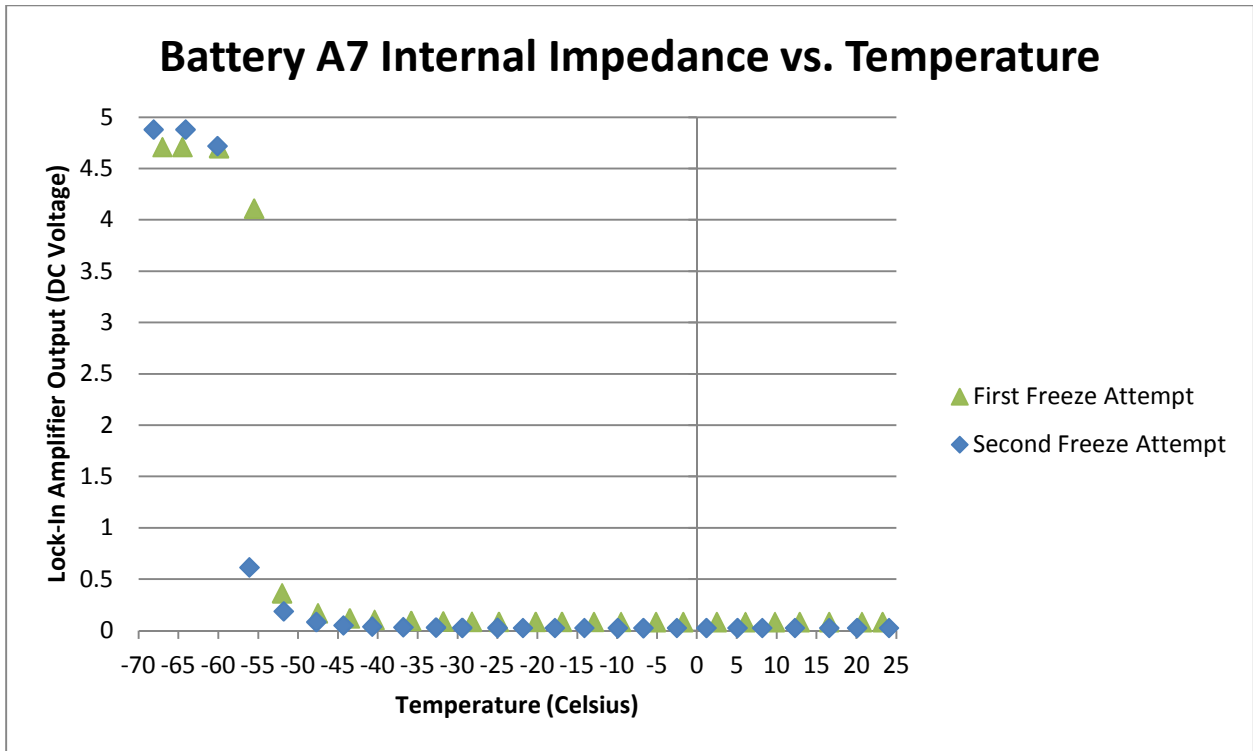


Figure 30: A7 Impedance vs. Temperature Test Results

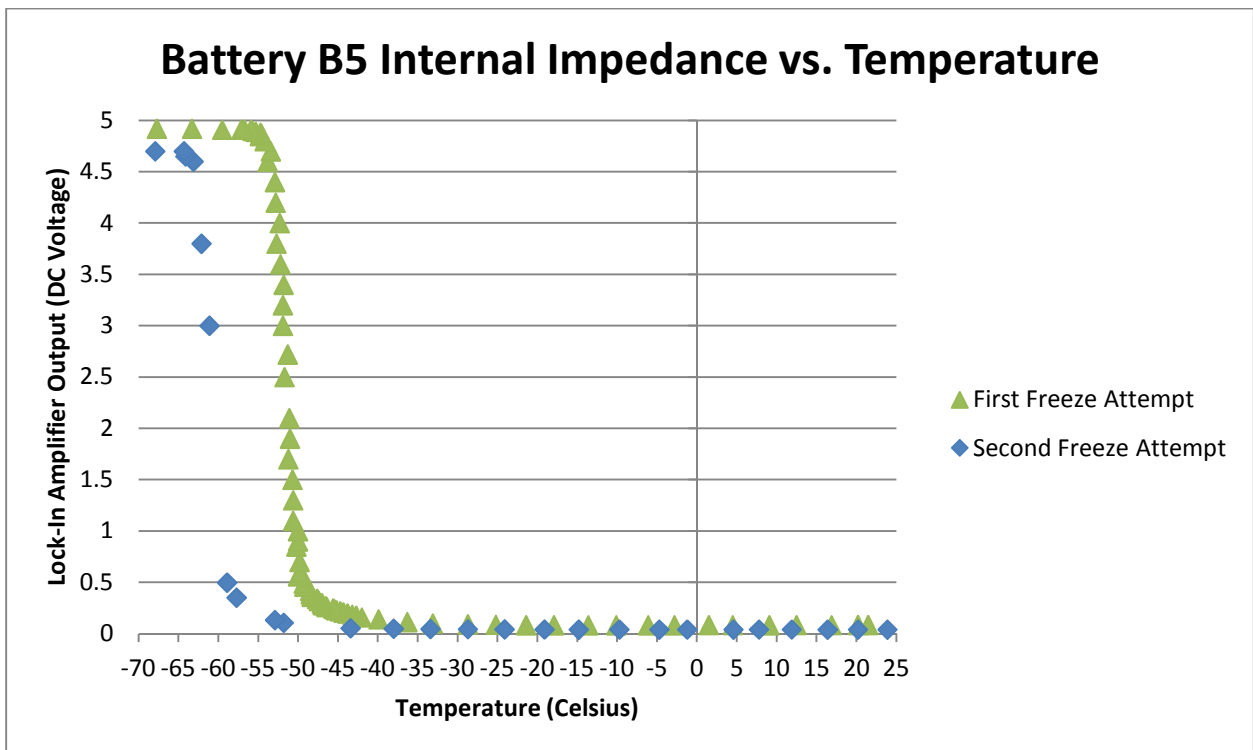


Figure 31: B5 Impedance vs. Temperature Test Results

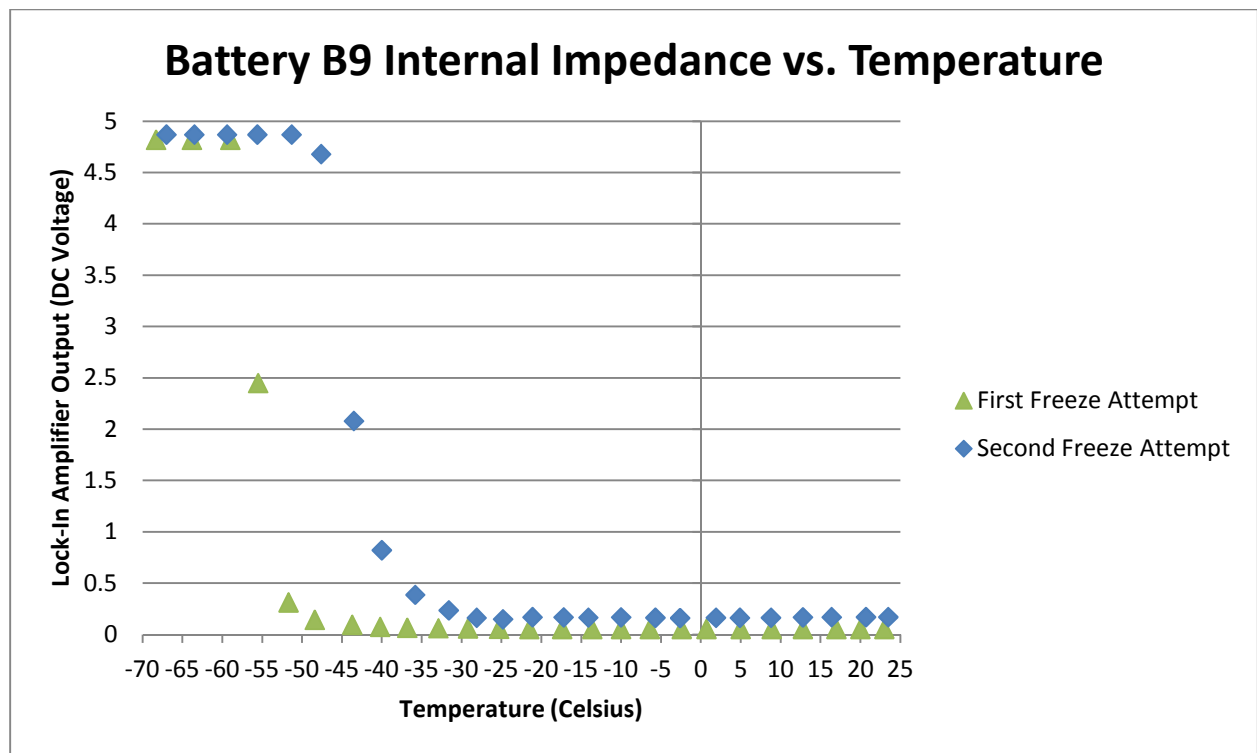


Figure 32: B9 Impedance vs. Temperature Test Results

Another important observation to make in the results can be seen in the following figures.

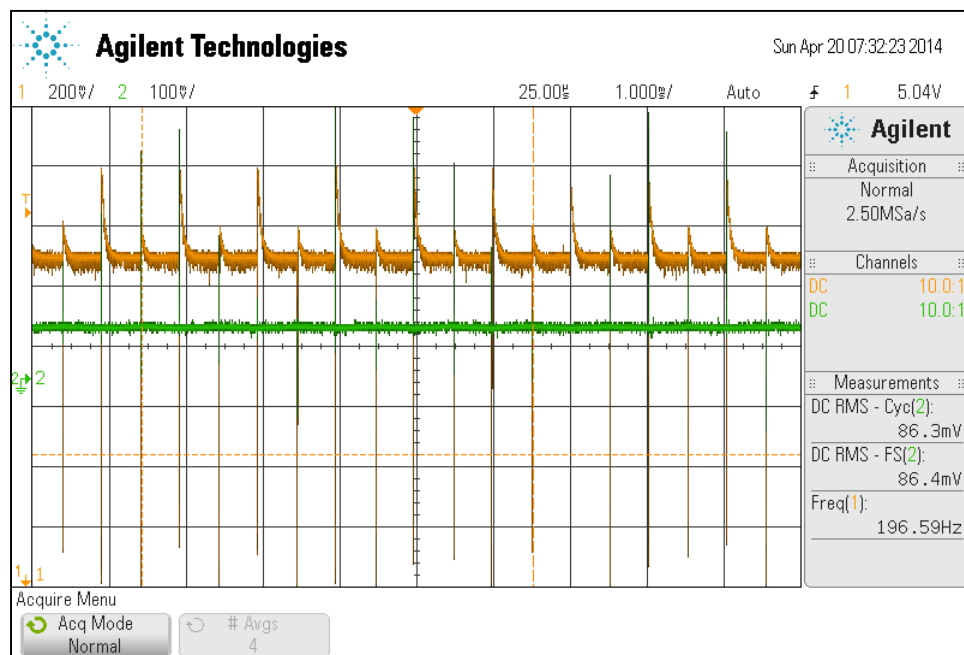


Figure 33: T = -28.8 °C - Ch.1 - Output of Discrete Amplifier; Ch. 2 - DC Output Voltage (Battery A7)

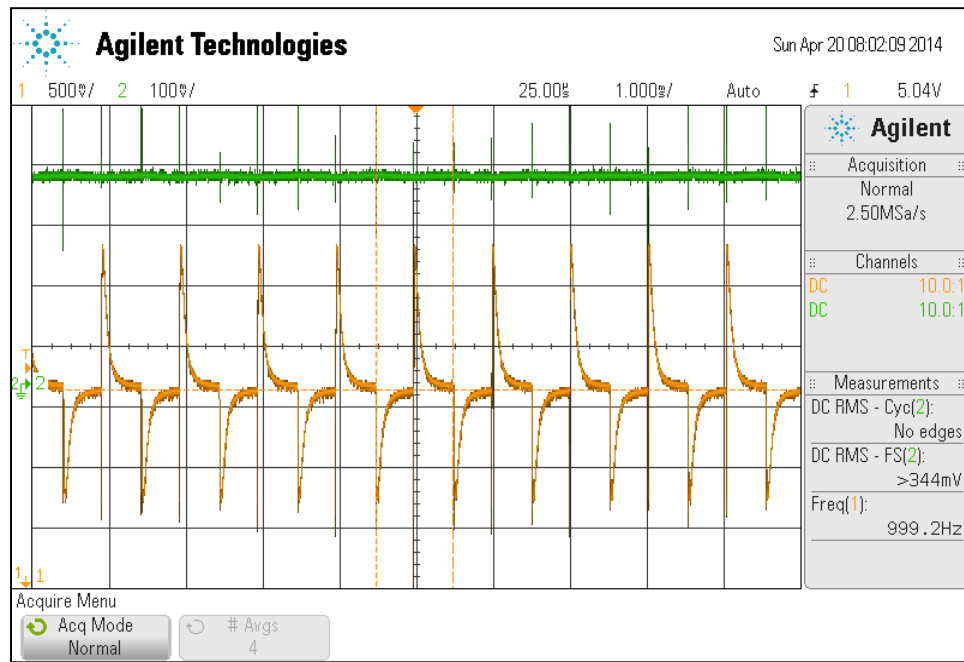


Figure 34: T = -52 °C - Ch. 1 - Output of Discrete Amplifier; Ch. 2 - DC Output Voltage (Battery A7)

As shown in Figure 33, before the battery begins to break, the output of the discrete amplifier does not behave as expected. Consider the following: if the internal impedance of a battery is modeled as a simple resistor, the voltage wiggle created from a square wave excitation circuit will also be a square wave. Thus, passing through a high-pass amplifier should result in the waveform shown in Ch.1 of Figure 19. However, this is not the case for the lithium-ion batteries we have tested. Every lithium-ion battery we tested expresses this "rectified" behavior, which serves as an indicator of the lithium-ion battery's complex internal impedance. Only when the battery begins to break does it express the predicted behavior, as shown in Figure 34. Thus, this characteristic can also serve as a visual indication of the battery's breaking point.

C. Discharge Tests

Purpose:

The discharge tests are a series of tests performed on 3100 mAh and 3400 mAh rated lithium-ion batteries. Batteries that have not undergone a freeze test and ones that have gone through one or two freeze tests are fully charged and discharged slowly with an electronic load at 1 A. The purpose of these discharge tests are to observe any effects that freezing has on the battery capacity, with fresh batteries that have not undergone any temperature tests used as a control and the batteries that have been frozen up to two times being tested.

Procedure:

To perform the tests, the test batteries are fully charged and connected to an electronic load that draws 1 A. The voltage across the battery is recorded every 15 minutes while current is being drawn. This test is performed on 2 batteries that have not undergone any temperature tests and 2 batteries that have been through freeze tests. These discharge tests are performed on batteries after they have undergone a temperature sweep test a single time. The discharge test is performed once again on a battery that has undergone two temperature sweep tests.

Results:

Figure 35 and Figure 36 show the results of the test for A-type (3400 mAh) and B-type (3100mAh) batteries respectively. For the A-Type discharge tests, the freeze tests did not have any adverse effect on the battery capacity. The fresh batteries and batteries that have undergone freeze tests lasted approximately 190 minutes under a 1 A load. At approximately 2.5 V, the voltage across the battery begins to lower to 0 V quickly due to the protection circuitry in the battery that prevents the battery from discharging at 2.5 V or lower. However, the data for the A7 first freeze discharge test is an outlier compared to the other tests results. This is most likely due to the battery having not been fully charged when the discharge test was conducted.

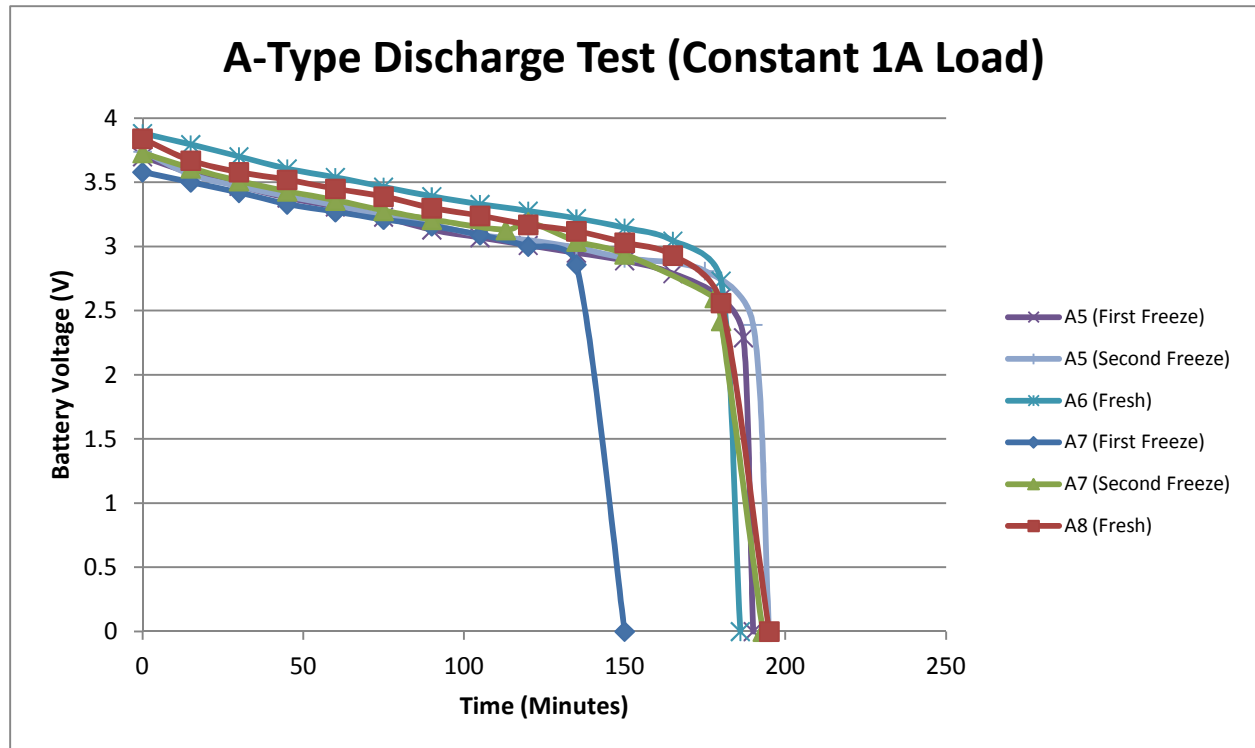


Figure 35: A-Type (3400 mAh rated) Discharge Test Results

The B-Type discharge tests demonstrated similar results, with batteries under all categories lasting approximately 200 minutes at 1 A load. The fresh battery B10 lasted 223 minutes which is 20 minutes longer than the average, but the other fresh battery B6 only lasted 203 minutes. Additionally, B5 and B9 after their 2nd freeze test lasted 212 and 210 minutes respectively. These results support the idea that freezing does not affect the charge capacity of the lithium-ion batteries even after they have undergone freeze tests. Even if these batteries are frozen down to -70 °C, their charge capacity will be relatively the same if charged back to full capacity.

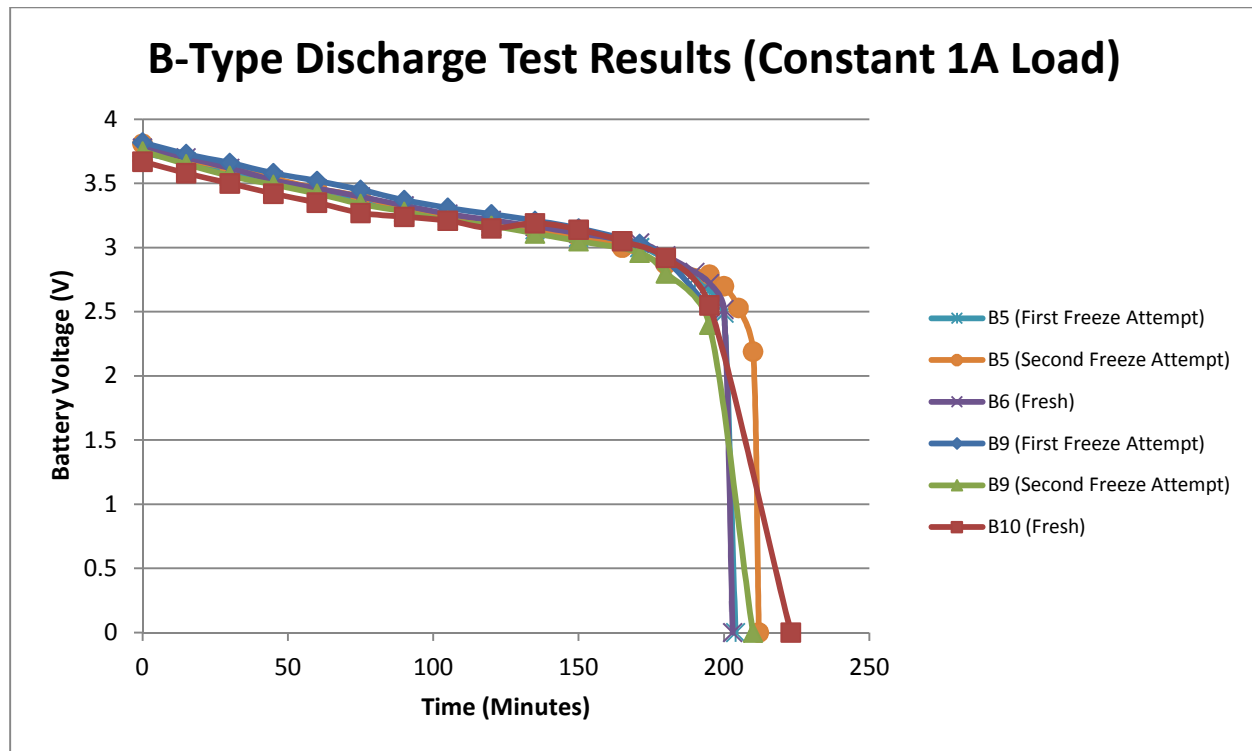


Figure 36: B-Type (3100 mAh rated) Discharge Test Results

D. Knee Tests

Purpose:

The knee tests are special battery tests performed to observe the effects of charge capacity in the batteries during a temperature sweep test. The prediction for these knee tests is that a battery that is fully charged and undergoes a temperature sweep test would have a failure point at a much lower temperature than a discharged battery that undergoes the same test. The charge capacity also affects the chemical composition of the battery, such as changing the pH level. Thus, this test is important in determining specific variables that affect the failure point of lithium-ion batteries.

Procedure:

Fully charged batteries are placed in the temperature chamber and swept from 25 °C towards -70 °C, but the test is stopped and the batteries are pulled out at the “knee” of their impedance measurement. It has been shown that the output voltage of the lock-in amplifier increases steadily at a certain temperature before rapidly increasing. This “knee” area is shown in the B5 temperature sweep tests as an example in Figure 37, marked as red circles. Once the battery has been pulled out of the chamber, the battery is discharged at 1 A with an electronic load until the voltage across the battery is approximately 2.5 V, right before the protection circuitry takes effect. The discharged battery is placed back into the temperature chamber and swept from 25 °C towards -70 °C again, with the expectation that the impedance measurement will increase more rapidly at a higher temperature. Batteries that have not undergone any freeze tests are chosen for these knee tests. Both A-Type and B-Type batteries are chosen for these tests to see if electric charge capacity is significant to impedance measurements.

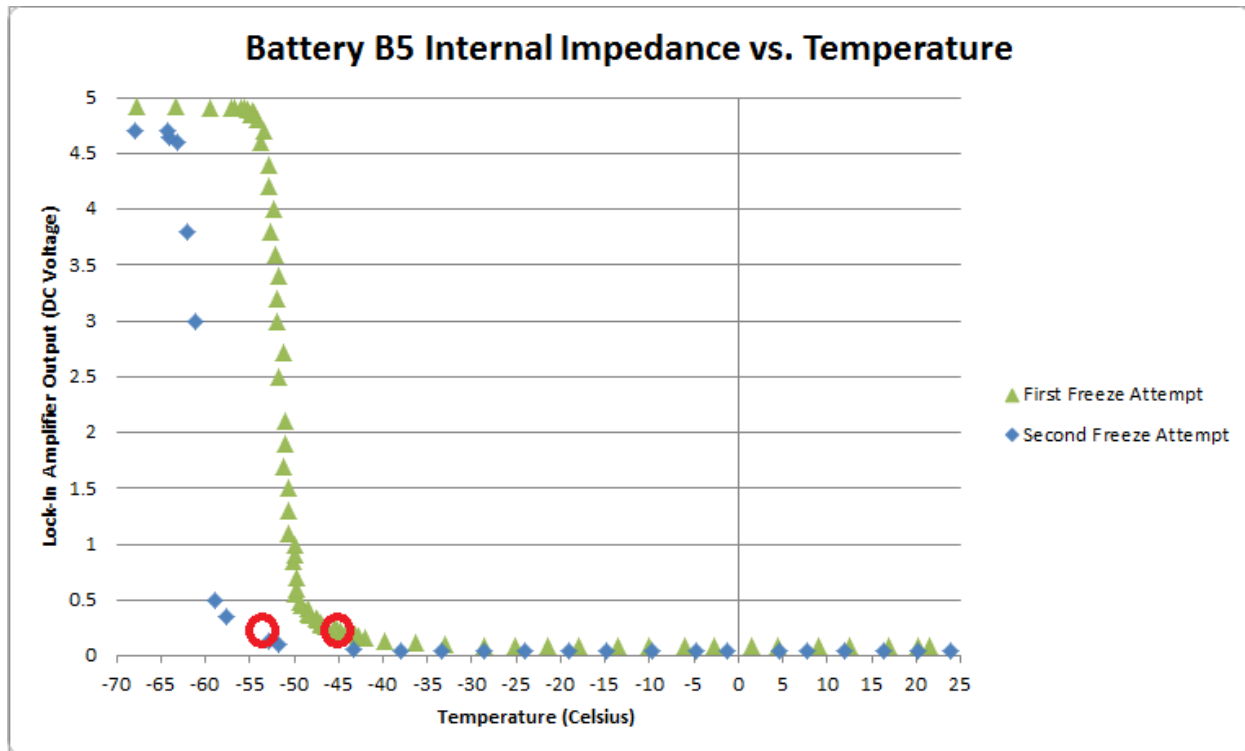


Figure 37: Example of "Knee" Area for Knee Test Results

Results:

Table 10 shows the results of the knee tests for A3 and B3 batteries, with both types displaying impedance spikes at -1 °C and 0 °C respectively. These temperatures are nearly 40 °C higher than the temperature at which they were removed from the temperature chamber. This supports the idea that the charge capacity and pH level of a battery affects the voltage measurements made from the lock-in amplifier at specific temperatures. Batteries that are almost completely discharged will have voltage measurements from the lock-in amplifier increase rapidly at higher temperatures. The conclusion drawn from this observation is that batteries will be much more susceptible to damage at cold temperatures if they are almost completely discharged.

Table 10: Knee Test Results

Battery	Temperature of Battery Removal (°C)	Temperature of Impedance Spike (°C)
A3	-37.2	-1
B3	-38	0

IX. Conclusion

The results of the impedance vs. temperature sweep tests show that the impedance of the batteries begin to increase dramatically at approximately -45°C for both 3400 mAh and 3100 mAh rated lithium-ion batteries. Also, if the batteries (both A-Type and B-Type) are not discharging and are allowed to reach a temperature of -70°C , the batteries can be recharged and reused with no apparent negative effects. This is supported by the discharge tests, that show the charge capacity of the batteries remaining relatively the same, regardless of freeze testing. The knee tests show that discharging the battery far below fully charged reduces the life span of the batteries at low temperature. The internal impedance of the batteries increase at an earlier temperature in comparison to fully charged batteries. Specifically, both A-Type and B-Type batteries have their impedance increase at approximately -38°C when fully charged, but when nearly discharged the increase in impedance occurs at $\sim 0^{\circ}\text{C}$. From the PCB freeze test, the lock-in amplifier fails at approximately -20°C due to the 555 timer no longer oscillating. Industrial or military grade discrete components would be necessary in order to withstand the low temperatures, as commercial grade components are not rated for such low temperatures.

For continued work on this project, the next step would be the design and testing of a control system that prevents the battery from discharging at temperatures lower than -45°C . Crucial components of this control system would include an analog-to-digital converter and a microcontroller. The ADC would translate the output DC voltage of the lock-in amplifier into a digital representation and a microcontroller can be used to detect the rise in battery internal impedance. The microcontroller would then be able to activate auxiliary control functions to prevent damage to the battery.

Another step would be to continue to explore and model the strange internal impedance of lithium-ion batteries, with its inherent "rectified" internal impedance. This project only models the battery's internal impedance as resistors and changing the model may result in different data that would help with the understanding of lithium-ion batteries from an internal impedance perspective. The new data may inspire new techniques to keep batteries functional.

X. References

- [1] R. Ford and C. Coulston, *Design for Electrical and Computer Engineers*, McGraw-Hill, 2007, p. 37.
- [2] *IEEE Std 1233, 1998 Edition*, p. 4 (10/36), DOI: 10.1109/IEEESTD.1998.88826
- [3] D.G. Vutetakis. "Batteries" in *The Avionics Handbook*, 2nd ed. C.R. Spitzer, Ed. Boca Raton: CRC Press LLC, 2001.
- [4] J. M. Hawkins and L. O. Barling, "Some aspects of battery impedance characteristics" in *The 17th International Telecommunications Energy Conference*, 1995, pp.271-276.
doi: 10.1109/INTLEC.1995.498964
- [5] H. Apgar *et al.* *Space Mission Analysis and Design*, 3rd ed. J.R. Wertz and W.J. Larson, Eds. Hawthorne: Microcosm Press, 2010.
- [6] H. J. Bergveld, W. S. Kruijt, and P. H.L. Notten, *Battery Management Systems: Design by Modeling*. Dordrecht, The Netherlands: Kluwer Academic Publishers, 2002.
- [7] V. Pop, H. J. Bergveld, D. Danilov, P. P.L. Regtien, and P. H.L. Notten, *Battery Management Systems: Accurate State-of-Charge Indication for Battery-Powered Applications*. Dordrecht, The Netherlands: Springer, 2008.
- [8] P. K. Homer *et al.*, "Battery Thermal Control Arrangement," U.S. Patent 5 310 141, May 10, 1994.
- [9] Texas Instruments Inc., "High-Performance Battery Monitor IC with Coulomb Counter, Voltage, and, Temperature Measurement," bq26221 datasheet, May 2004.
- [10] M. Coleman, C. K. Lee, C. Zhu, and W. G. Hurley, "State-of-Charge Determination from EMF Voltage Estimation: Using Impedance, Terminal Voltage, and Current for Lead-Acid and Lithium-Ion Batteries," *IEEE Trans. Ind. Electron*, vol. 54, no. 5, pp. 2550-2557, Oct. 2007.
- [11] A. Hammouche, E. Karden, and R. W. De Doncker, "Monitoring State-of-Charge of Ni-MH and Ni-Cd Batteries Using Impedance Spectroscopy," *Journal of Power Sources*, vol. 127, pp. 105-111, March 2004.
- [12] S. Piller, M. Perrin, and A. Jossen, "Methods for State-of-Charge Determination and Their Applications," *Journal of Power Sources*, vol. 96, pp. 113-120, June 2001.
- [13] *Tenney Junior Environmental Test Chamber Operation & Maintenance Manual*, Thermal Product Solutions, New Columbia, PA, 2010,

Appendix A – Senior Project Analysis

Project Title: Low Temperature Battery Monitoring and Control System – Lithium-Ion Low Temperature Case Study

Student's Name: Aaron Lee, Richard Tham, Ken Huynh

Student's Signature: (not filled out since electronic copy)

Advisor's Name: Dr. Prodanov, Dr. Dolan

Advisor's Initials: (not filled out since electronic copy)

Date: (not filled out since electronic copy)

1. Summary of Functional Requirements

The low temperature battery monitoring system monitors the health of batteries through internal impedance measurements while the batteries provide power to a load at from room temperature to -70° C. The system prototype assesses the feasibility of avoiding heating circuits for low-Earth-orbit (LEO) satellites and serves as a proof of concept. This project accomplishes the first half of the entire system, which monitors the health of batteries (Li-ion in this case) at low temperatures.

2. Primary Constraints

The primary challenge associated with this project is the low temperature condition. Many commercial devices can monitor battery health [9]. However, none operate at -70°C in addition to monitor the internal impedance while the battery provides power to a load. Thus, a different approach is needed. Additionally, the temperature range and internal physical dimensions of the temperature chamber limit both the testable temperature and the size of the implemented system and chosen battery. Lastly, funding is limited by the California Polytechnic State University Electrical Engineering Department Senior Project Fund of 200 USD per person. Therefore, having a three person group limits the total project cost to 600USD. As seen in Table 14, cost was a big issue due to having the majority of the costs consumed in the purchase of batteries. The cost of obtaining a temperature chamber is not a primary constraint because a temperature chamber already exists for testing. The last constraint is the time limit given on the project. Due to the nature of the senior project courses, the time given to work on the project is limited to approximately 1.5 quarters or approximately 18 weeks.

3. Economic

Many LEO satellites have systems that monitor the health of a battery in addition to actuating active heating elements to prevent damage to batteries. If the system designed for this project is successful, the monitoring system may provide insight into alternate methods of monitoring and maintaining battery health in LEO satellites.

Many current implementations of LEO satellite power systems include heating circuits to keep the battery pack and associated circuits functional. If an efficient solution is found, it may be considered in the future as a different approach in designing satellites. This changes the design process, manufacturing process, and the cost of the LEO satellites.

The project costs accrue throughout this project from the amount of batteries and PCBs ordered throughout this project. It is highly likely that both the system and the batteries will be damaged during testing. However, a low temperature chamber is available on campus for testing and mitigates the project costs. Furthermore, the advisers have existing batteries and a battery controller to help gain familiarity with battery characteristics. Overall, the total cost will be less than \$600 because of the existing equipment. This number is chosen since \$200 is allocated to each member of a project group via the senior project fund.

Table 11: Labor Cost Estimates

Labor Cost	Time (Hours)
Definition of Requirements and Specifications	66
Pre-Design State	54
Design Stage #1	84
Build Stage #1	8
Test Stage #1	54
Design Stage #2	72
Build Stage #2	8
Test Stage #2	96
Total	442
Labor Cost in USD (\$20/hr)	\$8840

Table 11 shows the preliminary cost estimates for this project. The labor cost includes a preliminary estimate of the total amount of hours required by the entire group (not per person). In the Definitions of Requirements and Specifications stage, we estimated two hours per person per week, which result in sixty-six hours after eleven weeks. With a total labor cost of 442 hours, the conversion of hours into USD at \$20/hr is \$8840.

Table 12: Parts Cost Estimates Breakdown (Estimate)

Parts Cost Breakdown (Likely Estimate)	Cost (USD)	Justification
Batteries	250	The largest cost due batteries replacements after characterization and testing
PCB	100	Approximate cost of designing a personal PCB and allowing for revisions.
Shielding	75	Cost for materials that may be used to insulate the battery.
Components/Parts	75	Cost for components and parts used in the active monitoring system .
Total	500	

Table 13: Parts Cost Estimates

Parts Cost	Cost (USD)
Most Optimistic Estimate	300
Most Likely Estimate	500
Most Pessimistic Estimate	650
Cost Estimate using Equation (6)	492

Table 12 shows a breakdown of the cost estimate and Table 13 presents a preliminary estimate of the total monetary cost for this project. This is determined using the \$600 senior project fund as a baseline (\$200 per person with 3 people in our group). Since we already have the low temperature chamber, several existing batteries, and a battery controller to measure different characteristics, most of the cost will come from ordering PCBs, additional batteries, insulation, etc [8].

This project only serves as a proof of concept, it does not worry about product development or maintenance.

Refer to Table 15 for the original estimated development time in the form of a Gantt chart.

After completing the project, the Gantt chart seen in Table 15 is not an accurate representation of the time required for the project. Characterization of the battery and the creation of the impedance monitoring system was greatly expanded which altered the actual schedule.

Table 14: Actual Parts Costs

Parts Cost Breakdown	Cost (USD)	Justification
Batteries	400	The largest cost due to ordering high quality batteries of various capacities.
PCB	100	Cost for six PCBs.
Components/Parts	100	Cost for components and parts used in the active monitoring system .
Total	600	

As seen in Table 14, the project was limited by the \$600 provided by the senior project fund. The initial battery purchase took 66% of the funding provided due to the high cost of quality batteries. Due to the change in scope of the project, shielding costs were removed and placed into the battery costs. Overall, the estimated costs were close to the actual costs due to the \$100 safety margin given in the estimated costs.

4. If manufactured on a commercial basis:

If this project is manufactured on a commercial basis, the estimated number of devices sold per year would be small because the low temperature battery monitoring and control system does not target the commercial industry; it is made for LEO satellite applications. LEO satellite applications are targeted because the time and resources provided do not allow enough research and testing into other applications.

Furthermore, because it is only a prototype, the robustness and efficiency of the prototype versus industry implementation will differ. The manufacturing costs of this prototype include the cost of the PCB and the various electrical components. Thus, the purchase price for one of these devices is significantly more expensive than the manufacturing cost because of the qualification process this device would need to go through due to the testing required. Ideally, this device will be part of a LEO satellite and will need to remain functional for the life cycle of a LEO satellite (approximately five years).

For industry implementations of this prototype, costs will differ because changes are needed to implement the system for industry applications. The prototype requires scaling to accommodate power requirements for spacecraft in addition to rigorous testing. Both scaling and testing increase manufacturing costs dramatically. Depending on the scaling and testing required for specific satellites, the manufactured cost of the system can vary dramatically.

5. Environmental

The manufacturing of this device requires all of the standard resources used to manufacture PCBs and electrical components, depleting those resources. Since this device will be used for space applications, it contributes to space littering in the Earth's orbit, which can impact the Earth's atmosphere. There already is a lot of "junk" floating around the Earth. However, although initially supporting space pollution, this project potentially helps limit the amount of needed LEO satellites because the deployed LEO satellites will be able to sustain themselves for longer periods of time. Furthermore, some of these devices can eventually re-enter the atmosphere and could be fatal to the surrounding environment if they do not disintegrate when entering Earth's atmosphere.

Batteries require natural resources that can include lithium, iron, zinc, carbon, alkaline, nickel, and mercury oxide. The factories and facilities that manufacture the batteries would generate waste in addition to the energy required to produce batteries. The chemical elements and metals listed earlier are extracted from the earth. Extracting those materials would directly deplete these natural resources. The process of extracting these resources can affect natural environments and any animals in that environment. However, if the LTBMCS is successful, it would reduce the need to reproduce a large amount of batteries because it would increase the lifespan of the batteries used for low temperature applications. as a result, it would counteract the harm to the natural environment during the battery manufacturing process.

6. Manufacturability

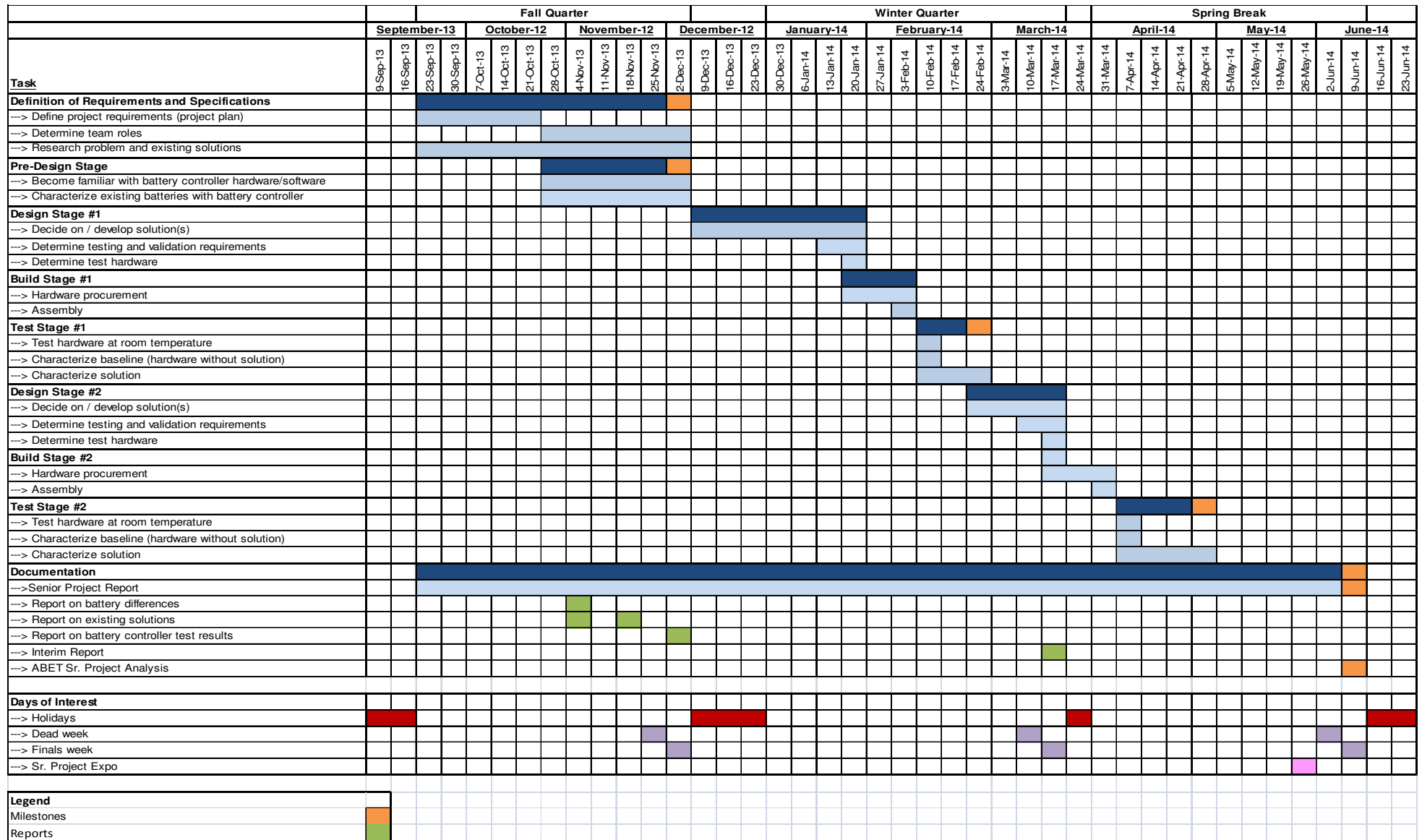
Manufacturing for this system consists of manufacturing PCBs and populating them with electrical components. However, they must be very precise components to ensure strong operation at low temperatures. Additionally, manufactured components must be designed to have functional ratings at low temperatures. All components and parts used must follow standard protocol for preventing electrostatic discharge damage when manufacturing, handling, installing, and testing of the system. Furthermore, special considerations are necessary to allow the PCBs to remain functional at lower temperatures either through special processes or special handling.

Another challenge of manufacturing this product is obtaining military or industrial grade battery cells. The prototype uses commercial grade battery cells and is likely to be the grade used for the final design. Unless a large amount of funding is obtained, this project will use commercial grade.

7. Sustainability

As stated before, this device is merely a prototype and serves as a proof of concept. However, if this device is actually implemented in a LEO satellite, it should not need maintenance for the life cycle of the satellite because there is no inexpensive way of accessing and repairing the satellite. Furthermore, as stated before, although this project potentially promotes the initial production of new satellites, it may limit the amount of satellites being produced long term because the new process may give the satellites a longer lifetime. as of now, there are no upgrades to be made because it is an open-ended research project. If the LTBMCS is successful in protecting and prolonging the condition of the batteries, then this project is highly sustainable. Additionally, the batteries are rechargeable, adding to the project's sustainability. The project would reduce the use of natural resources such as zinc, iron, nickel, etc. It would also reduce electrical waste because there is a lower amount of disposed batteries. The project can be improved with military grade or industrial grade batteries to increase the lifespan of the battery during any application of LTBMCS. The challenge of this upgrade is the high cost (in the range of \$1000-10000).

Table 15: Project Timeline (Gantt Chart)



8. Ethical

Satellites have always been controversial because of their spying capabilities. Although this device is not a satellite itself, it would be part of one and can contribute to unethical uses of the satellite. This would result in possible conflicts and bribery in order to secure the data obtained by the satellites, violating the IEEE Code of Ethics. Thus, their actions would support Psychological Egoism, where humans act in self-interest. Ethics is especially important in this project at a time where the United States has been accused and exposed of spying on their own citizens and other countries. This project is used to potentially help LEO satellites and can be potentially used to promote satellites and spying. Additionally, full documentation of the system is required when implementing satellites. The battery provides the main source of power for the satellite. Therefore, a failure in the battery system can cause de-orbit or collisions with other satellites. Collisions or de-orbit can also pose danger to the public and the environment. Thus, testing and documenting all actions are required in addition to full disclosure of all flaws in the system when testing and designing the system. The LTBMCS attempts to reduce the need to constantly replace damaged batteries from low temperatures. The project should aim to be ethical in that it reduces the electronic waste generated by batteries. If the project is successful, the LTBMCS can be further improved through the addition of higher grade batteries. However, it is possible for potential manufacturers of this system to use lower grade batteries in order to reduce costs. This negatively impacts the ethics of this system because the best and most efficient grade batteries are not being used.

9. Health and Safety

The chemicals inside the batteries are hazardous to humans, animals, and the environment. The batteries would need to be disposed of properly as electrical waste. The batteries also pose a fire hazard or explode if handled at improper temperatures or other conditions. Improper handling of the 28 V batteries can potentially cause electrocution as well.

There are no direct health and safety concerns associated with this project besides the standard health and safety concerns associated with manufacturing because this device will be implemented in a satellite orbiting the Earth and it is unlikely that the public will have direct contact with the system. However, one possible safety concern is the failure of the battery pack while a satellite is in orbit. The battery pack provides the main source of power for the satellite, and if failure occurs the satellite may de-orbit or collide with other satellites. This can cause additional space debris or possibly human harm if de-orbiting occurs and the entire satellite does not disintegrate during de-orbit.

10. Social and Political

The stakeholders in this project include the group members, the advisers Dr. Dolan and Dr. Prodanov, the Cal Poly Electrical Engineering Department, the United States of America, and other countries that have launched satellites or have the potential to launch them. In this case, Northrop Grumman has the most to gain from this project because they will have research to work with if this project produces results. If it is not successful, the only stakeholder to be negatively affected is the California Polytechnic State University Electrical Engineering Department. Northrop Grumman does not lose anything because the existing conditions will remain the same (no new implementations) but the department loses money that is obtained for the senior project fund. The LTBMCS is designed to improve the lifespan of batteries in low temperature conditions and would have impacts on both political and social issues. The main issue with batteries is that it becomes harmful electronic waste if disposed of improperly. There are public and political policies that enforce the disposal of electronic waste and regulate the use of the chemicals used to manufacture these batteries. The LTBMCS would promote these policies as the system would reduce the need for additional batteries. Additional political issues can be issues that arise from defense

companies due to their lobbying for contracts. Defense companies receive many contracts from the government, and political tension will arise if Northrop Grumman obtains a way to reduce the cost of launching satellites due to a new method of preserving batteries. Also, if the system is implemented in satellites, ITAR(International Traffic in Arms Regulations) must be met. The stakeholders would be the manufacturer of batteries and political/social parties that advocate for technology that reduces waste. While the project benefits waste reduction advocates, it could harm manufacturers of batteries. There would be a reduced need for manufacturing additional batteries due to the LTBMCS increasing the lifespan of the batteries.

11. Development

This project has taught me about equivalent circuit models and how basic electrical components can be used to model batteries[6]. Furthermore, I have learned about the different battery types and the existing techniques used to monitor them. For this project, a Lock-In amplifier was used to monitor the internal impedance of the battery. In order to design the Lock-In amplifier, understanding how the lock-in works was necessary. During characterization of batteries, the effects of low temperature on the impedance of batteries was measured and documented. Additionally, the software program called PCB Artist had to be learned in order to create and design the PCB.

Literature Search

- [1] R. Ford and C. Coulston, *Design for Electrical and Computer Engineers*, McGraw-Hill, 2007, p. 37
- [2] *IEEE Std 1233, 1998 Edition*, p. 4 (10/36), DOI: 10.1109/IEEESTD.1998.88826
- [3] D.G. Vutetakis. "Batteries" in *The Avionics Handbook*, 2nd ed. C.R. Spitzer, Ed. Boca Raton: CRC Press LLC, 2001.

This source was chosen because it provides a good overview of battery fundamentals, Lead-Acid batteries, Nickel-Cadmium batteries, and several battery applications.

This source has the authority to provide reliable information because, according to Google Scholar, it has been cited 92 times. Furthermore, the author has been the director of the Advanced Battery Technology group of Concorde Battery Corporation for almost 9 years. This company is a leading producer of specialty lead acid batteries. Since 1979, they have manufactured aircraft batteries and batteries for shipboard use by the U.S. Military.

- [4] J. M. Hawkins and L. O. Barling, "Some aspects of battery impedance characteristics" in *The 17th International Telecommunications Energy Conference*, 1995, pp.271-276. doi: 10.1109/INTLEC.1995.498964

This source was chosen because it provides insight on battery impedance characteristics, which is a quantity we are required to monitor.

This source has the authority to provide reliable information because, according to Google Scholar, it has been cited 22 times. This includes at least 5 IEEE articles and 2 patents. Furthermore, this research was done as part of Telstra Research Laboratories and they were a leading telecommunications research and development facility up until their closure in 2006. Furthermore, the author J. M. Hawkins has co-authored 13 papers, all of which have been presented at the International Telecommunications Energy Conference from 1994-2004.

- [5] H. Apgar *et al.* *Space Mission Analysis and Design*, 3rd ed. J.R. Wertz and W.J. Larson, Eds. Hawthorne: Microcosm Press, 2010.

This source was chosen because the goal of this project is to assess the feasibility of alternative solutions used for low-Earth-orbit satellites. Thus, this book provides in-depth examples of satellite designs and metrics related to different space missions at different altitudes, etc.

This source has the authority to provide reliable information because, according to Google Scholar, it has been cited 2116 times. The U.S. Department of Energy and Washington, D.C. also sponsor this source.

- [6] H. J. Bergveld, W. S. Kruijt, and P. H.L. Notten, *Battery Management Systems: Design by Modeling*. Dordrecht, The Netherlands: Kluwer Academic Publishers, 2002.

This source was chosen because it provides an overview and comparison of several battery types and provides methods for electrically modeling batteries. This will be useful for circuit simulations when we design and simulate the system.

This source has the authority to provide reliable information because, according to Google Scholar, is has been cited 146 times. Furthermore, it is research conducted by Philips Research, the research division of Royal Philips. Royal Philips, founded in 1891, is one of the largest electronics companies in the world. Philips Research is also one of the world's largest corporate research organizations with over 130,000 patents created.

- [7] V. Pop, H. J. Bergveld, D. Danilov, P. P.L. Regtien, and P. H.L. Notten, *Battery Management Systems: Accurate State-of-Charge Indication for Battery-Powered Applications*. Dordrecht, The Netherlands: Springer, 2008.

This source was chosen because it covers several methods for determining the state-of-charge of battery-powered applications. This senior project requires accurate means of determining the battery's health, which can take place in the form of state-of-charge.

This source has the authority to provide reliable information because, according to Google Scholar, it has been cited 111 times. Furthermore, it is research conducted by Philips Research, the research division of Royal Philips. Royal Philips, founded in 1891, is one of the largest electronics companies in the world. Philips Research is also one of the world's largest corporate research organizations with over 130,000 patents created. Furthermore, all of the authors have published numerous papers to IEEE conferences and journals.

- [8] P. K. Homer *et al.*, "Battery Thermal Control Arrangement," U.S. Patent 5 310 141, May 10, 1994.

This source was chosen because it provides insight on one aspect of batteries that we need to consider: thermal insulation of batteries for aircraft/satellite applications. Batteries' differing constructions play a vital role in their temperature changes. Furthermore, this senior project is geared towards low-Earth-orbit satellites.

This source has the authority to provide reliable information because this patent was originally assigned to General Electric Co. It is now assigned to Lockheed Martin Co.

- [9] Texas Instruments Inc., “High-Performance Battery Monitor IC with Coulomb Counter, Voltage, and, Temperature Measurement,” bq26221 datasheet, May 2004.

This source was chosen because it is a battery monitor similar to what we are trying to design and provides an established approach (i.e. coulomb counting).

This source has the authority to provide reliable information because it is an IC produced by Texas Instruments Inc. Texas Instruments is now the world's largest maker of analog components and is among the top 20 semiconductor producing companies in the world.

- [10] M. Coleman, C. K. Lee, C. Zhu, and W. G. Hurley, “State-of-Charge Determination from EMF Voltage Estimation: Using Impedance, Terminal Voltage, and Current for Lead-Acid and Lithium-Ion Batteries,” *IEEE Trans. Ind. Electron.*, vol. 54, no. 5, pp. 2550-2557, Oct. 2007.

This source was chosen because it provides a more updated approach on determining the state-of-charge (published in 2007).

This source has the authority to provide reliable information because, according to Google Scholar, it has been cited 99 times. of the 99, it has been cited by 60 IEEE publications and 3 other journal publications (*IET Renewable Power Generation*, *Journal of Power Sources*, and *Applied Energy*).

- [11] A. Hammouche, E. Karden, and R. W. De Doncker, “Monitoring State-of-Charge of Ni-MH and Ni-Cd Batteries Using Impedance Spectroscopy,” *Journal of Power Sources*, vol. 127, pp. 105-111, March 2004.

This source was chosen because it covers monitoring the state-of-charge of nickel cadmium batteries using impedance spectroscopy, an approach this senior project is currently considering.

This source has the authority to provide reliable information because, according to Google Scholar, it has been cited 36 times. Furthermore, the publisher is *Journal of Power Sources*, a peer-reviewed scientific journal that covers all aspects of electrochemical energy conversion and it has been publishing since 1976. Lastly, this article will provide updated and relevant information since it was published in 2004.

- [12] S. Piller, M. Perrin, and A. Jossen, “Methods for State-of-Charge Determination and Their Applications,” *Journal of Power Sources*, vol. 96, pp. 113-120, June 2001.

This source was chosen because it provides information on different methods for state-of-charge determination and their particular applications. This is relevant because this senior project is trying to determine the most efficient method for monitoring the battery's health.

This source has the authority to provide reliable information because, according to Google Scholar, it has been cited 449 times. Furthermore, the publisher is *Journal of Power Sources*, a peer-reviewed scientific journal that covers all aspects of electrochemical energy conversion and it has been publishing since 1976. Lastly, this article will provide updated and relevant information since it was published in 2001.

- [13] *Tenney Junior Environmental Test Chamber Operation & Maintenance Manual*, Thermal Product Solutions, New Columbia, PA, 2010,

This source is useful because it is the Manual/Datasheet for the test chamber used for this project.

It is needed because it will provide instructions and specifications of the test chamber.

This source has authority because the manufacturer of the test chamber creates and provides the manual/datasheet. They designed and built the product, therefore they would have the most information regarding the product.